Electronic Supplementary Information

Unlocking the PIP-box: A peptide library reveals interactions that drive high affinity binding to human PCNA

Aimee J. Horsfall, Beth A. Vandborg, Wioleta Kowalczyk, Theresa Chav, Denis B. Scanlon, Andrew D. Abell* and John B. Bruning*

ABBREVIATIONS

ACN, acetonitrile; **Ala (A),** alanine; **Arg (R),** arginine; **Asn (N),** asparagine; **Asp (D),** aspartic acid; **Boc,** tert-butoxycarbonyl; **Cys (C),** cysteine; **DCM**, dichloromethane; **DEAE,** diethylethanolamine; **DIC,** *N,N'*-diisopropylcarbodiimide; **DIPEA**, *N,N'*-diisopropylethylamine; **DMF**: *N,N'*-dimethylformamide; **DODT**: 2,2′-(ethylenedioxy)diethanethiol; **DTT,** dithiothreitol; **E. Coli,** Escherichia Coli; **EDC,** 1-ethyl-3-(3-diethylaminopropyl)carbodiimide; **EDTA,** ethylenediaminetetraacetic acid; **ESI-TOF,** Electrospray Ionisation Time of Flight; **Fmoc**, 9-fluorenylmethoxycarbonyl; **Gln (Q),** glutamine; **Glu (E),** glutamic acid; **Gly (G),** glycine; **HATU**, (1-[bis(dimethylamino)methylene]-1H-1,2,3-triazolo[4,5-b]pyridinium 3-oxide hexafluorophosphate; **HEPES,** 4-(2-hydroyethyl)-1-piperazineethanesulfonic acid; **His (H),** histidine; **HOBt,** 1-hydroxybenzotriazole; **HPLC**: High Performance Liquid Chromatography; **HRMS:** High Resolution Mass Spectrometry; **Ile (I),** isoleucine; **IPTG,** isopropyl β-D-1-thiogalactopyranoside; **LB:** Lennox broth; **LCMS**: Liquid Chromatography Mass Spectrometry; **Leu (L),** leucine; **Lys (K),** lysine; **Met (M),** methionine; **NHS,** N-hydroxysuccinimide; **Pbf**: 2,2,4,6,7-pentamethyldihydrobenzofuran-5-sulfonyl; **PCNA,** Proliferating Cell Nuclear Antigen; **Phe (F),** phenylalanine; **Pro (P),** proline; **RP-HPLC**: Reverse-Phase High Performance Liquid Chromatography; **SDS,** Sodium Dodecyl Sulfate; **Ser (S),** serine; **SPPS**: Solid-Phase Peptide Synthesis; **tBu**: tert-butyl; **TFA:** trifluoroacetic acid; **Thr (T),** threonine; **TIPS**: triisopropylsilane; **TNBS,** 2,4,6-trinitrobenzenesulfonic acid (picrylsulfonic acid); **Tris,** trisaminomethane; **Trp (W),** tryptophan; **Trt,** trityl; **Tyr (Y),** tyrosine; **Val (V),** valine;

TABLE OF CONTENTS

SYNTHESIS & CHARACTERISATION OF PEPTIDES **2**
Table S1: Peptide characterisation data 4
SPR: **5**
Table S2: Peptide SPR data against hPCNA. 5
COCRYSTAL EXPERIMENTS **6**
Table S3: Data collection and refinement statistics of hPCNA bound with p21$_{\mu}$, and hPCNA bound with p21$_{\mu}$-F150Y. 6
Figure S1: Co-crystal structure of p21$_{\mu}$ bound to PCNA monomer. 7
Table S4: Secondary Interaction Summary for co-crystal structure of p21$_{\mu}$ with hPCNA. 7
Figure S2: Co-crystal structure of p21$_{\mu}$-F150Y bound to PCNA monomer. 8
Table S5: Secondary Interaction Summary for co-crystal structure of p21$_{\mu}$-F150Y with hPCNA. 8
COMPUTATIONAL MODELLING OF PCNA MONOMERS BOUND TO P21μ PEPTIDES **9**
Figure S3: Computationally modelled structure of p21$_{\mu}$-M147I on the PIP-box binding site of a hPCNA monomer. 9
Table S6: Secondary Interaction Summary for computationally modelled structured of p21$_{\mu}$-M147I with hPCNA. 9
Figure S4: Computationally modelled structure of p21$_{\mu}$- FY150/151YF on the PIP-box binding site of a hPCNA monomer. 10
Table S7: Secondary Interaction Summary for computationally modelled structured of p21$_{\mu}$-FY150/151YF with hPCNA. 10
Figure S5: Computationally modelled structure of p21$_{\mu}$-S146R on the PIP-box binding site of a hPCNA monomer. 11
Table S8: Secondary Interaction Summary for computationally modelled structured of p21$_{\mu}$-S146R with hPCNA. 11
Figure S6: Computationally modelled structure of p21$_{\mu}$- D149E on the PIP-box binding site of a hPCNA monomer. 12
Table S9: Secondary Interaction Summary for computationally modelled structured of p21$_{\mu}$-D149E. 12
Figure S7: Computationally modelled structure of p21$_{\mu}$- pol δ_{p66} on the PIP-box binding site of a hPCNA monomer. 13
Table S10: Secondary Interaction Summary for computationally modelled structured of p21$_{\mu}$-pol δ_{p66} with hPCNA. 13
Figure S8: Computationally modelled structure of p21$_{\mu}$-Pogo on the PIP-box binding site of a hPCNA monomer. 14
Table S11: Secondary Interaction Summary for computationally modelled structured of p21$_{\mu}$-Pogo with hPCNA. 14
Figure S9: Computationally modelled structure of p21$_{\mu}$- PARG on the PIP-box binding site of a hPCNA monomer. 15
Table S12: Secondary Interaction Summary for computationally modelled structured of p21$_{\mu}$-PARG with hPCNA. 15
Figure S10: Computationally modelled structure of p21$_{\mu}$-pol ι on the PIP-box binding site of a hPCNA monomer 16
Table S13: Secondary Interaction Summary for computationally modelled structured of p21$_{\mu}$-pol ι with hPCNA. 16
Figure S11: Computationally modelled structure of p21$_{\mu}$-RFC on the PIP-box binding site of a hPCNA monomer. 17
Table S14: Secondary Interaction Summary for computationally modelled structured of p21$_{\mu}$-RFC with hPCNA. 17
Figure S12: Computationally modelled structure of p21$_{\mu}$-RD1 on the PIP-box binding site of a hPCNA monomer. 18
Table S15: Secondary Interaction Summary for computationally modelled structured of p21$_{\mu}$-RD1 with hPCNA 18
Figure S13: Computationally modelled structure of p21$_{\mu}$-RD2 on the PIP-box binding site of a hPCNA monomer. 19
Table S16: Secondary Interaction Summary for computationally modelled structured of p21$_{\mu}$-RD2 with hPCNA. 19
Figure S14: Computationally modelled structure of p21$_{\mu}$-RD3 on the PIP-box binding site of a hPCNA monomer 20
Table S17: Secondary Interaction Summary for computationally modelled structured of p21$_{\mu}$-RD3 with hPCNA. 20
ANALYSIS OF STRUCTURES **21**
Table S18: Root-mean-squared deviation (RMSD) values of modified p21$_{\mu}$. 21
Table S19: Buried Surface Area (BSA) of modified p21$_{\mu}$. 21
COMPARISON OF STRUCTURES TO NATIVE SEQUENCES **22**
Figure S15: Overlaid structures of p21μ:PIP-box hybrid (blue) and native PIP-box peptide (yellow) 22
Table S20: Root-mean-squared deviation (RMSD) values of alternative PIP-box modified peptides 23
Table S21: Number of interactions for p21μ:hybrid peptides compared to native analogues 23
REFERENCES **24**

SYNTHESIS & CHARACTERISATION OF PEPTIDES

Unless otherwise indicated, all starting materials were purchased from commercial sources and used without further purification. All peptides were synthesised by the Fmoc/tBu solid-phase peptide synthesis using one of three protocols detailed below, with all L-amino acids (unless otherwise specified) purchased from Chem-Impex Int'l.: Fmoc-Ala-OH, Fmoc-Arg(Pbf)-OH, Fmoc-Asp(tBu)-OH, Fmoc-Asn(Trt)-OH, Fmoc-Cys(Trt)-OH, Fmoc-Gln(Trt)-OH, Fmoc-Glu(tBu)-OH, Fmoc-Gly-OH, Fmoc-His(Trt)-OH, Fmoc-Ile-OH, Fmoc-Leu-OH, Fmoc-Lys(Boc)-OH, Fmoc-Met-OH, Fmoc-Thr(tBu)-OH, Fmoc-Tyr(tBu)-OH, Fmoc-Trp(Boc)-OH, Fmoc-Ser(tBu)-OH, Fmoc-Phe-OH, Fmoc-Pro-OH, Fmoc-Val-OH. Peptides were subsequently cleaved from the resin (and simultaneously globally deprotected) and purified per '*Cleavage from solid-support, isolation & purification'*. Purity of all compounds was confirmed by analytical RP-HPLC on an Agilent 1260 HPLC equipped with a Phenomenex Luna C18(2) column (250 x 4.6 mm) over a gradient of 5-50% B (15 min) and visualised at 220 nm. High-resolution mass spectra were collected using an Agilent 6230 ESI-TOF via direct injection in ACN with 0.1% formic acid as the running buffer. Characterisation data for all peptides in recorded in Table S1.

Peptide Synthesis:

All peptides were synthesised using one of the following methods, excepting ten peptides that were purchased from Shanghai Royobiotech at >95% purity, with purity & identity confirmed on receipt by HPLC and HRMS. *Purchased peptides:* $p21_{\mu}$-M147L, $p21_{\mu}$-M147A, $p21_{\mu}$-M147W, $p21_{\mu}$-M147V, $p21_{\mu}$-Q144D, $p21_{\mu}$-Q144M, $p21_{\mu}$-Q144S, $p21_{\mu}$-FY150/151YF, $p21_{\mu}$-p15, and $p21_{\mu}$-Cdt1.

Liberty Blue Synthesis:

All peptides were synthesised by the Fmoc/tBu solid-phase peptide synthesis protocol on a CEM Liberty Blue Automated Microwave Peptide Synthesiser (CEM Corp., Matthews, NC, USA) using the standard manufacturer's conditions. The peptides were assembled on 0.1 mmol scale on Chem Impex Rink Amide AM resin (0.47 mmol/g) or Mimotopes Rink Amide resin (0.456 mmol/g). The resin was initially swollen in DCM (10 mL, 15 min) and then the resin washed with DMF (2 × 5 mL) and transferred to the microwave reaction vessel. The resin-bound Fmoc-groups were deprotected with a mixture of 20% piperidine and 0.1 M OxymaPure in DMF using the standard microwave deprotection method with a maximum temperature of 90°C. Couplings were performed with Fmoc-protected amino-acids (0.2 M in DMF, 5 equiv), OxymaPure (1 M in DMF, 5 equiv) and DIC (0.5 M in DMF, 5 equiv) under the 'Standard Coupling' microwave method with a maximum temperature of 90°C, except for coupling of Fmoc-His(Trt)-OH which was coupled using a maximum 50°C 10 min coupling procedure; and Fmoc-Arg(Pbf)-OH which used the default 'Arginine Double Coupling' microwave method which included two couplings steps – the first at room temperature and the second at a maximum of 75°C. Following assembly of the desired sequence the N-terminal protecting group was removed. The resin was then removed from the synthesiser, washed with DCM (3 × 5 mL) and then diethyl ether (3 × 5 mL) and air dried with suction. The peptides were then cleaved from the resin according to the protocol '*Cleavage from solid-support, isolation & purification'* detailed below.

Peptides synthesised by this method: $p21_{139\text{-}160}$‡, $p21_{\mu}$, $p21_{\mu}$-F150Y, $p21_{\mu}$-Y151F, $p21_{\mu}$-F150H, $p21_{\mu}$-M147I

‡ The N-terminal glycine was subjected to a standard double coupling cycle as initial syntheses indicated incomplete incorporation at this position. Please note, this sequence is particularly prone to aspartimide formation.

Prelude Synthesis:

Peptides were assembled using a Protein Technologies Prelude® Peptide synthesiser. Chem Impex Rink Amide resin (0.1 mmol, 0.47 mmol/g) was preswollen in DCM for 15 min, and washed with DMF (3 × 10 mL, 1.5 min). The Fmoc-protecting group was removed by treatment with 20% piperidine (3 × 8 mL, 7 min) and the resin washed with DMF (5 × 10 mL, 1.5 min). An amino-acid was then coupled by addition of the required Fmoc-amino-acid (7.5 equiv, 150 mM in DMF), HCTU (5 equiv, 0.5 M in DMF) and DIPEA (10 equiv, 1 M in DMF) and bubbled with nitrogen for 15 min before the solution was drained, and a fresh coupling solution added to the resin and bubbled with nitrogen for 10 min. The solution was drained and the resin washed with DMF (4 × 8 mL, 1.5 min). Fmoc deprotection and coupling steps were repeated until the desired sequence was achieved, and the final *N*-terminal Fmoc group deprotected. The resin was then removed from the synthesiser and washed

with DCM (3 × 5 mL) and then diethyl ether (3 × 5 mL) and air dried with suction. The peptides were then cleaved from the resin according to the protocol '*Cleavage from solid-support, isolation & purification'* detailed below.

Peptides synthesised by this method: $p21_{\mu}$-Q144K, $p21_{\mu}$-Q144N, $p21_{\mu}$-T145K, $p21_{\mu}$-T145R, $p21_{\mu}$-S146K, $p21_{\mu}$-S146R, $p21_{\mu}$-T148D, $p21_{\mu}$-T148E, $p21_{\mu}$-D149E, $p21_{\mu}$-TS145/146KK, $p21_{\mu}$-TS145/146RK, $p21_{\mu}$-TS145/145KR, $p21_{\mu}$-TS145/146RR, $p21_{\mu}$-TD148/149EE, $p21_{\mu}$-TS148/149DE, $p21_{\mu}$-RNaseH2B, $p21_{\mu}$-MCMT, $p21_{\mu}$-pol λ, $p21_{\mu}$-pol β, $p21_{\mu}$-pol δ_{p66}, $p21_{\mu}$-FEN1, $p21_{\mu}$-RFC, $p21_{\mu}$-RecQ5, $p21_{\mu}$-DNALig1, $p21_{\mu}$-WRN, $p21_{\mu}$-XPG, $p21_{\mu}$-Cdt2 $p21_{\mu}$-Pogo, $p21_{\mu}$-pol η, $p21_{\mu}$-pol κ.

Manual Synthesis

Rink Amide PL resin (0.1 mmol, 322 mg, 0.31 mmol/g, Agilent) was swollen in 1:1 DMF/DCM (15 mL) for 15 min. The Fmoc-protecting group was removed by treatment of the resin with a solution of 20% piperidine and 0.1 M HOBt in DMF (5 mL) for 15 min. The solution was drained and the resin washed with DMF (3 × 5 mL). Amino-acid couplings were achieved by addition of a solution of Fmoc-protected amino-acid (5 equiv), HATU (5 equiv) and DIPEA (10 equiv) in DMF (5 mL), to the resin and stirred intermittently for 1 h. The solution was drained and the resin washed with DMF (5 × 5 mL). The *N*-terminal Fmoc-protecting group was removed by treatment of the resin with a solution of 20% piperidine and 0.1 M HOBt in DMF (5 mL) for 10 min, the solution was drained and the resin washed with DMF (5 × 5 mL). A TNBS test* was used to verify each coupling (negative/colourless) and deprotection (positive/red) step, with steps repeated as necessary. Successive couplings and Fmoc-deprotections were repeated to achieve the desired sequence. The resin was washed with DCM (3 × 5 mL) and then diethyl ether (3 × 5 mL) and air dried with suction. The peptides were then cleaved from the resin according to the protocol '*Cleavage from solid-support, isolation & purification'* detailed below.

* *TNBS Test:* A small spatula of swollen resin taken out and 1 drop each of TNBS (100 µL 5% w/v in H_2O added to 900 µL of DMF) and DIPEA solutions (100 µL in 900 µL of DMF) added and allowed to develop for 1 min. Clear/yellow beads indicated no free amine (negative), while red/orange beads showed free amine was present (positive).

Peptides synthesised by this method: $p21_{\mu}$-pol ι, $p21_{\mu}$-PARG, $p21_{\mu}$-RD1, $p21_{\mu}$-RD2, $p21_{\mu}$-RD3.

Cleavage from solid-support, isolation & purification

Following complete assembly of the peptide and deprotection of the final Fmoc group, the peptides were subsequently cleaved from the resin and the side-chain protecting groups simultaneously globally deprotected by treatment of the resin with 92.5/2.5/2.5/2.5 TFA:TIPS:DODT:H_2O (5 mL) for 2 hours. The cleavage mixture was pipetted from the resin and concentrated under a stream of nitrogen to 0.5-1 mL. The peptide was then precipitated by addition of diethyl ether (10 mL) and the mixture cooled to -20°C. The precipitate was pelleted by centrifugation (7600 rpm, 10 min), and the supernatant decanted. The pellet was dried under a nitrogen stream, and then dissolved in 1:1 ACN/H_2O, before being syringe filtered (0.2 µm) and lyophilised to yield the crude peptide as a fluffy white powder. The peptides were purified by semi-preparative RP-HPLC on a Gilson GX-Prep system using a Phenomenex Luna C18(2) column (10 × 250 mm), over a linear ACN/H_2O gradient optimised for each peptide sample. RP-HPLC solvents were (A) H_2O with 0.1% TFA and (B) ACN with 0.1% TFA. The product containing fractions were pooled and lyophilised. The identity of the final compounds was confirmed by High Resolution Mass Spectrometry on an Agilent 6230 ESI-TOF LCMS. Purity of the peptides was confirmed by analytical RP-HPLC on an Agilent 1260 HPLC equipped with a Phenomenex Luna C18(2) column (250 × 4.6 mm) over a gradient of 5-50% B (15 min) and visualised at 220 nm. Characterisation data for all peptides in recorded in Table S1.

Table S1: Peptide characterisation data. All peptides are C-terminally amidated.

Name	Sequence	Mw	MF	M+ Calc	$[M+4]^{4+}$ Calc	ESI+ $[M+4]^4$ Found	Purity % (220 nm)
$p21_{\mu}$ (141-155)	^{141}KRRQTSMTDFYHSKR	1940.20	$C_{82}H_{134}N_{30}O_{23}S_1$	1938.9959	485.7570	485.7566	96.3
p21 (139-160)	^{139}GRKRRQTSMTDFYHSKRRLIFS	2770.20	$C_{120}H_{197}N_{43}O_{31}S_1$	2769.4722	693.3760	693.3793	97.4
$p21_{\mu}$-Q144D	KRR**D**TSMTDFYHSKR	1927.16	$C_{81}H_{131}N_{29}O_{24}S_1$	1925.9642	482.4991	482.5010	98.8
$p21_{\mu}$-Q144M	KRR**M**TSMTDFYHSKR	1943.27	$C_{82}H_{135}N_{29}O_{22}S_2$	1941.9778	486.5024	486.5020	98.9
$p21_{\mu}$-Q144S	KRR**S**TSMTDFYHSKR	1899.15	$C_{80}H_{131}N_{29}O_{23}S_1$	1897.9693	475.5003	475.4999	97.3
$p21_{\mu}$-Q144K	KRR**K**TSMTDFYHSKR	1940.24	$C_{83}H_{138}N_{30}O_{22}S_1$	1939.0323	485.7661	485.7658	93.4
$p21_{\mu}$-Q144N	KRR**N**TSMTDFYHSKR	1926.18	$C_{81}H_{132}N_{30}O_{23}S_1$	1924.9802	482.2531	482.2527	90.7
$p21_{\mu}$-T145K	KRRQ**K**SMTDFYHSKR	1967.27	$C_{84}H_{139}N_{31}O_{22}S_1$	1966.0432	492.5188	492.5206	90.2
$p21_{\mu}$-T145R	KRRQ**R**SMTDFYHSKR	1995.28	$C_{84}H_{139}N_{33}O_{22}S_1$	1994.0493	499.5203	499.5215	91.0
$p21_{\mu}$-S146K	KRRQT**K**MTDFYHSKR	1981.30	$C_{85}H_{141}N_{31}O_{22}S_1$	1980.0588	496.0227	496.0235	87.0
$p21_{\mu}$-S146R	KRRQT**R**MTDFYHSKR	2009.31	$C_{85}H_{141}N_{33}O_{22}S_1$	2008.0650	503.0243	503.0250	94.0
$p21_{\mu}$-TS145/146KK	KRRQ**KK**MTDFYHSKR	2008.37	$C_{87}H_{146}N_{32}O_{21}S_1$	2007.1061	3+: 670.0492	670.3799	91.3
$p21_{\mu}$-TS145/146RK	KRRQ**RK**MTDFYHSKR	2036.38	$C_{87}H_{146}N_{34}O_{21}S_1$	2035.1122	509.7861	509.7864	93.0
$p21_{\mu}$-TS145/146KR	KRRQ**KR**MTDFYHSKR	2036.38	$C_{87}H_{146}N_{34}O_{21}S_1$	2035.1122	509.7861	509.7859	91.9
$p21_{\mu}$-TS145/146RR	KRRQ**RR**MTDFYHSKR	2064.39	$C_{87}H_{146}N_{36}O_{21}S_1$	2063.1184	516.7876	516.7877	90.9
$p21_{\mu}$-M147I	KRRQTS**I**TDFYHSK	1765.98	$C_{77}H_{124}N_{26}O_{22}$	1764.9383	442.2426	442.2419	99.1
$p21_{\mu}$-M147L	KRRQTS**L**TDFYHSKR	1922.16	$C_{83}H_{136}N_{30}O_{23}$	1921.0395	481.2679	481.2672	99.8
$p21_{\mu}$-M147A	KRRQTS**A**TDFYHSKR	1880.08	$C_{80}H_{130}N_{30}O_{23}$	1878.9925	470.7561	470.7556	99.2
$p21_{\mu}$-M147W	KRRQTS**W**TDFYHSKR	1995.22	$C_{88}H_{135}N_{31}O_{23}$	1994.0347	499.5167	499.5161	99.5
$p21_{\mu}$-M147V	KRRQTS**V**TDFYHSKR	1908.14	$C_{82}H_{134}N_{30}O_{23}$	1907.0238	477.7640	477.7632	98.5
$p21_{\mu}$-T148D	KRRQTSM**D**DFYHSKR	1954.19	$C_{82}H_{132}N_{30}O_{24}S_1$	1952.9751	489.2518	489.2514	91.5
$p21_{\mu}$-T148E	KRRQTSM**E**DFYHSKR	1968.21	$C_{83}H_{134}N_{30}O_{24}S_1$	1966.9908	492.7557	492.7562	90.4
$p21_{\mu}$-D149E	KRRQTSMT**E**FYHSKR	1954.23	$C_{83}H_{136}N_{30}O_{23}S_1$	1953.0115	489.2609	489.2620	88.5
$p21_{\mu}$-TD148/149EE	KRRQTSM**EE**FYHSKR	1982.24	$C_{84}H_{136}N_{30}O_{24}S_1$	1981.0065	496.2596	496.2595	89.4
$p21_{\mu}$-TS148/149DE	KRRQTSM**DE**FYHSKR	1968.21	$C_{83}H_{134}N_{30}O_{24}S_1$	1966.9908	492.7557	492.7555	90.1
$p21_{\mu}$-F150H	KRRQTSMTD**H**YHSKR	1930.16	$C_{79}H_{132}N_{32}O_{23}S_1$	1928.9864	483.2546	483.2542	94.4
$p21_{\mu}$-F150Y	KRRQTSMTD**Y**YHSKR	1956.20	$C_{82}H_{134}N_{30}O_{24}S_1$	1954.9908	489.7557	489.7552	93.8
$p21_{\mu}$-Y151F	KRRQTSMTDF**F**HSKR	1924.20	$C_{82}H_{134}N_{30}O_{22}S_1$	1923.0010	481.7582	481.7576	94.2
$p21_{\mu}$-FY150/151YF	KRRQTSMTD**YF**HSKR	1940.20	$C_{82}H_{134}N_{30}O_{23}S_1$	1938.9959	485.7570	485.7589	98.1
$p21_{\mu}$-DNALig1	KRR**QRSIMSFF**HSKR	1963.32	$C_{85}H_{143}N_{33}O_{19}S_1$	1962.0959	491.5320	491.5311	98.2
$p21_{\mu}$-FEN1	KRR**QGRLDDFF**HSKR	1945.20	$C_{84}H_{137}N_{33}O_{21}$	1944.0667	487.0247	487.0241	99.2
$p21_{\mu}$-Pogo	KRR**QKKITDYF**HSKR	1990.32	$C_{88}H_{148}N_{32}O_{21}$	1989.1497	498.2954	498.2965	98.0
$p21_{\mu}$-XPG	KRR**QLRIDSFF**HSKR	1973.29	$C_{87}H_{145}N_{33}O_{20}$	1972.1344	494.0416	494.0409	99.1
$p21_{\mu}$-MCMT	KRR**QTTITSHF**HSKR	1882.14	$C_{80}H_{136}N_{32}O_{21}$	1881.0558	471.2719	471.2714	93.9
$p21_{\mu}$-p15	KRR**QKGIGEFF**HSKR	1873.18	$C_{83}H_{137}N_{31}O_{19}$	1872.0707	469.0257	469.0265	96.5
$p21_{\mu}$-Cdt1	KRR**QRRVTDFF**HSKR	2016.33	$C_{87}H_{146}N_{36}O_{20}$	2015.1514	504.7959	504.7954	94.8
$p21_{\mu}$-pol δ_{p66}	KRR**QVSITGFF**HSKR	1846.15	$C_{82}H_{136}N_{30}O_{19}$	1845.0598	462.2729	462.2727	99.2
$p21_{\mu}$-RecQ5	KRR**QNLIRHFF**HSKR	2022.37	$C_{90}H_{148}N_{36}O_{18}$	2021.1772	506.3024	506.3019	99.2
$p21_{\mu}$-WRN	KRR**QWKLLRDF**HSKR	2053.42	$C_{92}H_{153}N_{35}O_{19}$	2052.2082	514.0600	514.0593	99.3
$p21_{\mu}$-PARG	KRR**DSKITDHF**HSKR	1910.16	$C_{81}H_{136}N_{32}O_{22}$	1909.0507	478.2707	478.2705	98.4
$p21_{\mu}$-pol β	KRR**QLQKVHF**HSKR	1847.18	$C_{81}H_{139}N_{33}O_{17}$	1846.1027	462.5337	462.5330	96.5
$p21_{\mu}$-pol λ	KRR**SVPVLELF**HSKR	1851.21	$C_{83}H_{143}N_{29}O_{19}$	1850.1115	463.5359	463.5353	92.4
$p21_{\mu}$-pol ι	KRR**KGLIDYYL**HSKR	1932.29	$C_{87}H_{146}N_{30}O_{20}$	1931.1330	483.7913	483.7919	87.6
$p21_{\mu}$-pol κ	KRR**KHTLDIFF**HSKR	1968.32	$C_{89}H_{146}N_{32}O_{19}$	1967.1442	492.7941	492.7939	93.5
$p21_{\mu}$-RFC_{p14}	KRR**MDIRKFF**HSKR	1904.30	$C_{84}H_{142}N_{32}O_{17}S_1$	1903.0951	476.7818	476.7813	93.4
$p21_{\mu}$-RNaseH2B	KRR**MKSIDTFF**HSKR	1936.29	$C_{85}H_{142}N_{30}O_{20}S_1$	1935.0737	484.7764	484.7761	97.7
$p21_{\mu}$-Cdt2	KRR**MRKICTYF**HSKR	2009.46	$C_{87}H_{149}N_{33}O_{18}S_2$	2008.1198	503.0380	503.0390	93.8
$p21_{\mu}$-pol n	KRR**MQTLESFF**HSKR	1950.28	$C_{85}H_{140}N_{30}O_{21}S_1$	1949.0530	488.2713	488.2719	96.6
$p21_{\mu}$-RD1	KRR**QRKMEDYY**HSKR	2080.39	$C_{88}H_{146}N_{34}O_{23}S_1$	2079.1021	520.7835	520.7836	91.0
$p21_{\mu}$-RD2	KRR**QTRITEYF**HSKR	2005.30	$C_{87}H_{145}N_{33}O_{22}$	2004.1242	502.0389	502.0396	97.1
$p21_{\mu}$-RD3	KRR**QKRITEYY**HSKR	2048.39	$C_{89}H_{150}N_{34}O_{22}$	2047.1664	512.7994	512.8001	92.3

SPR:

Table S2: Peptide SPR data against hPCNA. Top Conc is the highest concentration of 8x 1 in 2 dilutions used to calculate the steady state affinity. K_D is the affinity constant. SE, standard fitting error; On/Off, indicate times for contact and dissociation phases of each run. All peptides are C-terminally amidated.

Name	Sequence	ε_{205}*	Top Conc (nM)	Affinity K_D (nM)	K_D SE (nM)	χ^2	On/Off (s)
p21μ (141-155)	^{141}KRRQTSMTDFYHSKR	67860	500	12.3	0.598	0.196	30/60
p21 (139-160)	^{139}GRKRRQTSMTDFYHSKRRLIFS	98620	50	4.319	1.31	10.9	60/90
p21μ-Q144D	KRR**D**TSMTDFYHSKR	67460	2000	714	30.4	0.126	40/60
p21μ-Q144M	KRR**M**TSMTDFYHSKR	69290	5000	1544	159	1.57	40/60
p21μ-Q144S	KRR**S**TSMTDFYHSKR	67460	5000	1032	116	2.07	40/60
p21μ-Q144K	KRR**K**TSMTDFYHSKR	67460	5000	1123	148	4.19	40/60
p21μ-Q144N	KRR**N**TSMTDFYHSKR	67860	5000	772	117	3.07	40/60
p21μ-T145K	KRRQ**K**SMTDFYHSKR	67860	2000	98.05	10.8	2.58	40/60
p21μ-T145R	KRRQ**R**SMTDFYHSKR	69210	1000	88.51	13.2	2.97	40/60
p21μ-S146K	KRRQT**K**MTDFYHSKR	67860	300	12.97	1.55	0.520	60/90
p21μ-S146R	KRRQT**R**MTDFYHSKR	69210	100	4.297	1.35	6.26	60/90
p21μ-TS145/146KK	KRRQ**KK**MTDFYHSKR	67860	300	20.18	4.80	6.70	60/90
p21μ-TS145/146RK	KRRQ**RK**MTDFYHSKR	69210	300	17.30	4.66	7.94	60/90
p21μ-TS145/146KR	KRRQ**KR**MTDFYHSKR	69210	300	37.00	11.0	9.63	60/90
p21μ-TS145/146RR	KRRQ**RR**MTDFYHSKR	70560	30	1.833	0.453	5.80	60/90
p21μ-M147I	KRRQTS**I**TDFYHSK	66030	200	11.1	0.258	0.0251	40/60
p21μ-M147L	KRRQTS**L**TDFYHSKR	66030	200	20.49	1.75	0.784	40/60
p21μ-M147A	KRRQTS**A**TDFYHSKR	66030	20000	7591	626	1.43	40/60
p21μ-M147W	KRRQTS**W**TDFYHSKR	86430	5000	3566	165	0.274	40/60
p21μ-M147V	KRRQTS**V**TDFYHSKR	66030	500	29.29	1.83	0.326	40/60
p21μ-T148D	KRRQTSM**D**DFYHSKR	67860	2000	96.47	7.32	0.477	40/60
p21μ-T148E	KRRQTSM**E**DFYHSKR	67860	200	77.40	2.62	0.0533	60/90
p21μ-D149E	KRRQTSMT**E**FYHSKR	67860	500	12.67	1.4	0.387	60/90
p21μ-TD148/149EE	KRRQTSM**EE**FYHSKR	67860	1000	48.52	1.16	0.0475	60/90
p21μ-TD148/149DE	KRRQTSM**DE**FYHSKR	67860	2000	345.8	2.67	0.273	60/90
p21μ-F150H	KRRQTSMTD**H**YHSKR	64460	1000	159.0	62.8	0.119	40/60
p21μ-F150Y	KRRQTSMTD**Y**YHSKR	65340	300	20.2	0.424	0.0286	40/60
p21μ-Y151F	KRRQTSMTDF**F**HSKR	70380	300	10.61	1.48	0.721	60/90
p21μ-FY150/151YF	KRRQTSMTD**YF**HSKR	67860	30	2.175	0.531	3.01	60/90
p21μ-DNALig1	KRR**QRSIMSFF**HSKR	71730	250	40.74	9.20	3.42	60/90
p21μ-FEN1	KRR**QGRLDDFF**HSKR	69900	2000	165.6	2.07	1.67	40/60
p21μ-Pogo	KRR**QKKITDYF**HSKR	66030	100	8.816	3.30	6.73	60/90
p21μ-XPG	KRR**QLRIDSFF**HSKR	69900	200	16.39	4.81	11.2	60/90
p21μ-MCMT	KRR**QTTITSHF**HSKR	65150	2000	106.0	24.4	5.32	40/60
p21μ-p15	KRR**QKGIGEFF**HSKR	68550	2000	234.0	42.4	5.21	40/60
p21μ-Cdt1	KRR**QRRVTDFF**HSKR	71250	150	8.760	2.22	10.1	40/60
p21μ-pol δ_{p66}	KRR**QVSITGFF**HSKR	68550	1000	123.7	4.24	3.21	40/60
p21μ-RecQ5	KRR**QNLIRHFF**HSKR	75500	20000	>40000**			
p21μ-WRN	KRR**QWKLLRDF**HSKR	81700	2000	1155	67.3	0.952	40/60
p21μ-PARG	KRR**DSKITDHF**HSKR	64750	2000	90.03	18.4	2.38	40/60
p21μ-pol β	KRR**QLQKVHF**HSKR	62770	20000	5732	822	18.6	40/60
p21μ-pol λ	KRR**SVPVLELF**HSKR	59550	20000	8144	766	4.81	40/60
p21μ-pol ι	KRR**KGLIDYYL**HSKR	63110	1500	111.2	5.41	0.0710	60/90
p21μ-pol κ	KRR**KHTLDIFF**HSKR	73350	10000	3296	353	6.62	40/60
p21μ-RFC_{p14}	KRR**MDIRKFF**HSKR	68550	1000	145.2	34.5	6.42	40/60
p21μ-Cdt2	KRR**MRKICTYF**HSKR	69500		NS***			
p21μ-pol η	KRR**MQTLESFF**HSKR	70380	10000	2537	745	10.2	40/60
p21μ-RNAseH2B	KRR**MKSIDTFF**HSKR	69980	2000	640.4	51.1	0.851	40/60
p21μ-RD1	KRR**QRKMEDYY**HSKR	66690	100	8.152	1.27	1.51	40/60
p21μ-RD2	KRR**QTRITEYF**HSKR	67380	50	1.118	0.330	2.40	60/90
p21μ-RD3	KRR**QKRITEYY**HSKR	64860	200	6.70	1.58	3.96	40/60

* Determined using online calculator, from Anthis 2013 (1)
** Peptide bound very non-specifically to protein where the RU significantly exceeded the expected maximum and a K_D could not be determine.
*** Peptide bound significantly to the reference cell of sensor chip such that a K_D could not be determined

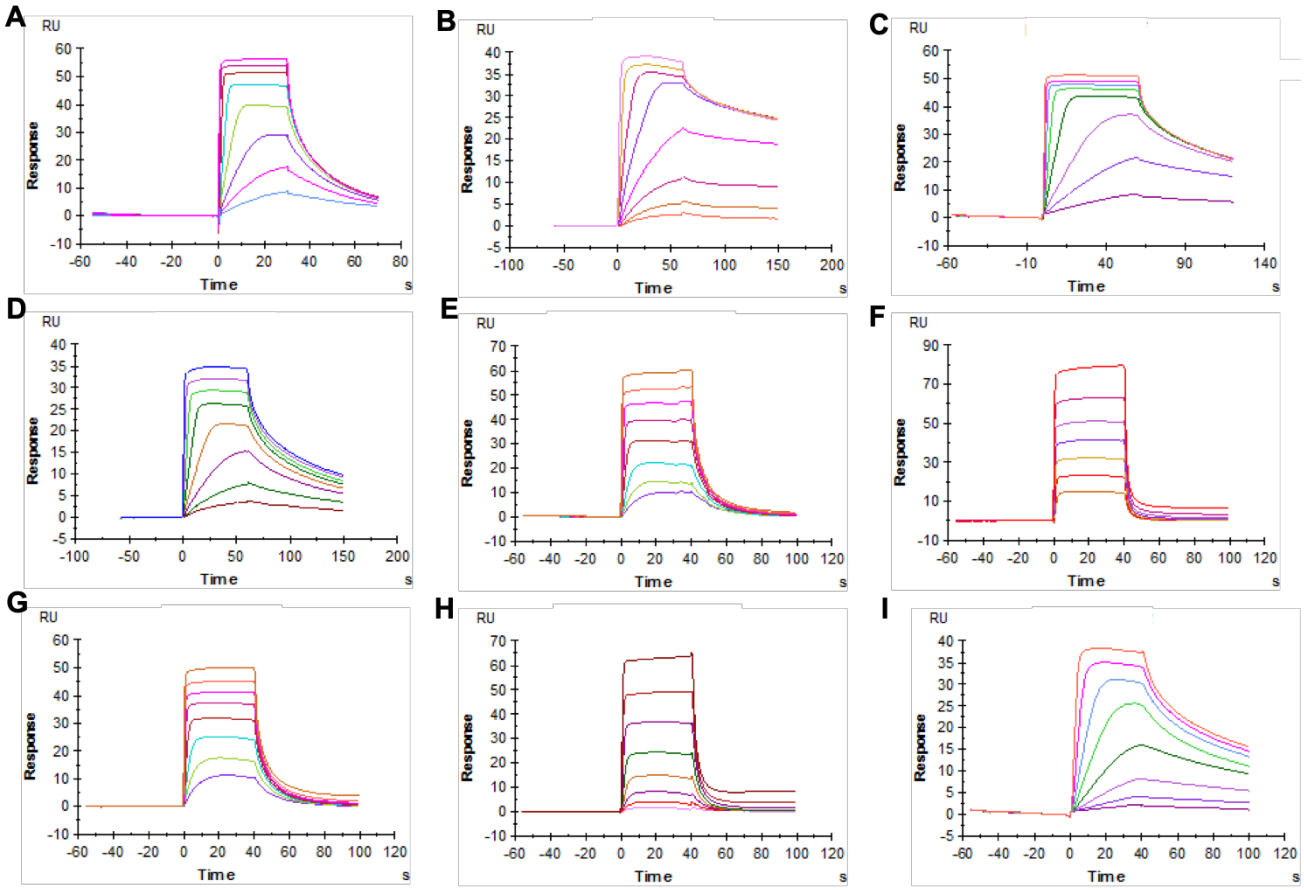

Figure S1: Representative sample of SPR sensorgrams. **A** p21μ **B** p21μ-S146R **C** p21μ-FY150/151YF **D** p21μ-Y151F **E** p21μ-FEN1 **F** p21μ-pol η **G** p21μ-PARG **H** p21μ-RNaseH2B **I** p21μ-RD1

COCRYSTAL EXPERIMENTS

Table S3: Data collection and refinement statistics of hPCNA bound with p21μ (RCSB PDB ID: 7KQ1), and hPCNA bound with p21μ-F150Y (RCSB PDB ID: 7KQ0). Statistics for the highest-resolution shell are shown in parentheses.

PDB ID	**7KQ1**	**7KQ0**
Wavelength	0.9537	0.9537
Resolution range	41.09 - 3.3 (3.418 - 3.3)	41.15 - 2.4 (2.486 - 2.4)
Space group	P 32 2 1	P 3
Unit cell	136.66 136.66 104.005 90 90 120	142.563 142.563 41.03 90 90 120
Unique reflections	17208 (1689)	32881 (3598)
Multiplicity	19.9 (18.2)	10.7 (11.1)
Completeness (%)	99.83 (99.64)	90.13 (99.94)
Mean I/sigma(I)	10.45 (0.91)	40.58 (13.50)
[a] R-merge	0.2823 (4.453)	0.04334 (0.1841)
[b] Rpim	0.065 (0.755)	0.014 (0.570)
CC1/2	0.999 (0.469)	1 (0.987)
Reflections used in refinement	17192 (1684)	32881 (3598)
Reflections used for R-free	1716 (171)	2031 (224)
[c] R-work	0.2419 (0.3591)	0.1537 (0.2023)
[d] R-free	0.2685 (0.3618)	0.2011 (0.2813)
Number of non-hydrogen atoms	6084	6086
macromolecules	6084	5976
Protein residues	816	807
RMS(bonds)	0.003	0.004
RMS(angles)	0.69	0.68
Ramachandran favoured (%)	94.78	98.10
Ramachandran allowed (%)	4.73	1.64
Ramachandran outliers (%)	0.50	0.25
Rotamer outliers (%)	0.00	8.80
Clashscore	8.80	3.15
Average B-factor	108.50	32.34

[a] $R_{merge} = \Sigma |I - < I >|/\Sigma I$.

[b] $Rpim = \Sigma h\,[1/(n_h - 1)]^{1/2}\,\Sigma i|<I_h> - I_{h,i}|/\Sigma_h\,\Sigma_i\,I_{h,i}$ (2)

[c] $R_{work} = \Sigma|F_o - F_c|/\Sigma|F_o|$ for all data excluding data used to calculate R_{free}.

[d] $R_{free} = \Sigma|F_o - F_c|/\Sigma|F_o|$, for all data.

Table S4: Secondary Interaction Summary for co-crystal structure of p21$_\mu$ with hPCNA (PDB ID: 7KQ1) calculated using the RING server. Only peptide chain interactions reported (chains B, D and F). Interactions reported are an average of the number of interactions observed for the three chains. RING session ID: 5ef50f2b0e9f94078ea226bd

		Intermolecular			Intramolecular		
	Residue	**VDW**	**H-Bond**		**VDW**	**H-Bond**	**Total**
FI	141	0	0		0	0	
	142	0.67	0		0	0	
	143	0	0.67		0	0	
PIP-box	* **144**	1.67	0		0	0	
	145	2.33	1.00		0.67	0.33	
	146	0.67	0.33		0.33	1.00	
	* **147**	6.67	1.00		0.33	1.67	
	148	0.33	0		0	0	
	149	0	0		0	0	
	* **150**	2.67	0.00		0	0	
	* **151**	2.00	0.67		0	0	
FI	152	1.00	1.00		0	0	
	153	1.67	0.33		0	0	
	154	0.67	1.00		0	0	
	155	0	0		0	0	
	Total	20.3	6.0		1.3	3.0	30.67
	PIP-box	16	3		1	3	23.67
	Flanking (FI)	4	3		0	0	7
	Conserved (*) PIP-box residues	11.00	1		0	2	14.00
	Non-conserved PIP-box residues	3.33	1.33		1.00	1.33	7.00
	Other: Intermolecular pi-stack between F-Tyr151 to E-Tyr133, and D-Tyr151 to C-Tyr250						

Table S5: Secondary Interaction Summary for co-crystal structure of p21$_\mu$-F150Y with hPCNA (PDB ID: 7KQ0) calculated using the RING server. Only peptide chain interactions reported (chains B, D and F). Interactions reported are an average of the number of interactions observed for the three chains. RING session ID: 5f595dab0e9f94078ea22f07

		Intermolecular			Intramolecular		
	Residue	**VDW**	**H-Bond**		**VDW**	**H-Bond**	**Total**
FI	141	0	0		0	0	
	142	1	0		0	0	
	143	0	1		0	0	
PIP-box	* **144**	1	0		0	0	
	145	1	1		0	1	
	146	1	0		1	0	
	* **147**	3	1		2	1	
	148	1	0		0	0	
	149	0	0		0	0	
	* **150**	2	0		0	0	
	* **151**	2	0		0	0	
FI	152	0	1		0	0	
	153	0	0		0	0	
	154	0	0		0	0	
	155	1	0		0	0	
	Total	13.0	4.0		2.67	2.67	22.33
	PIP-box	11	2		3	3	18.33
	Flanking (FI)	2	2		0	0	4
	Conserved (*) PIP-box residues	6.67	1		2	1	10.67
	Non-conserved PIP-box residues	2.00	0.67		1.00	1.33	5.00
	Other:						

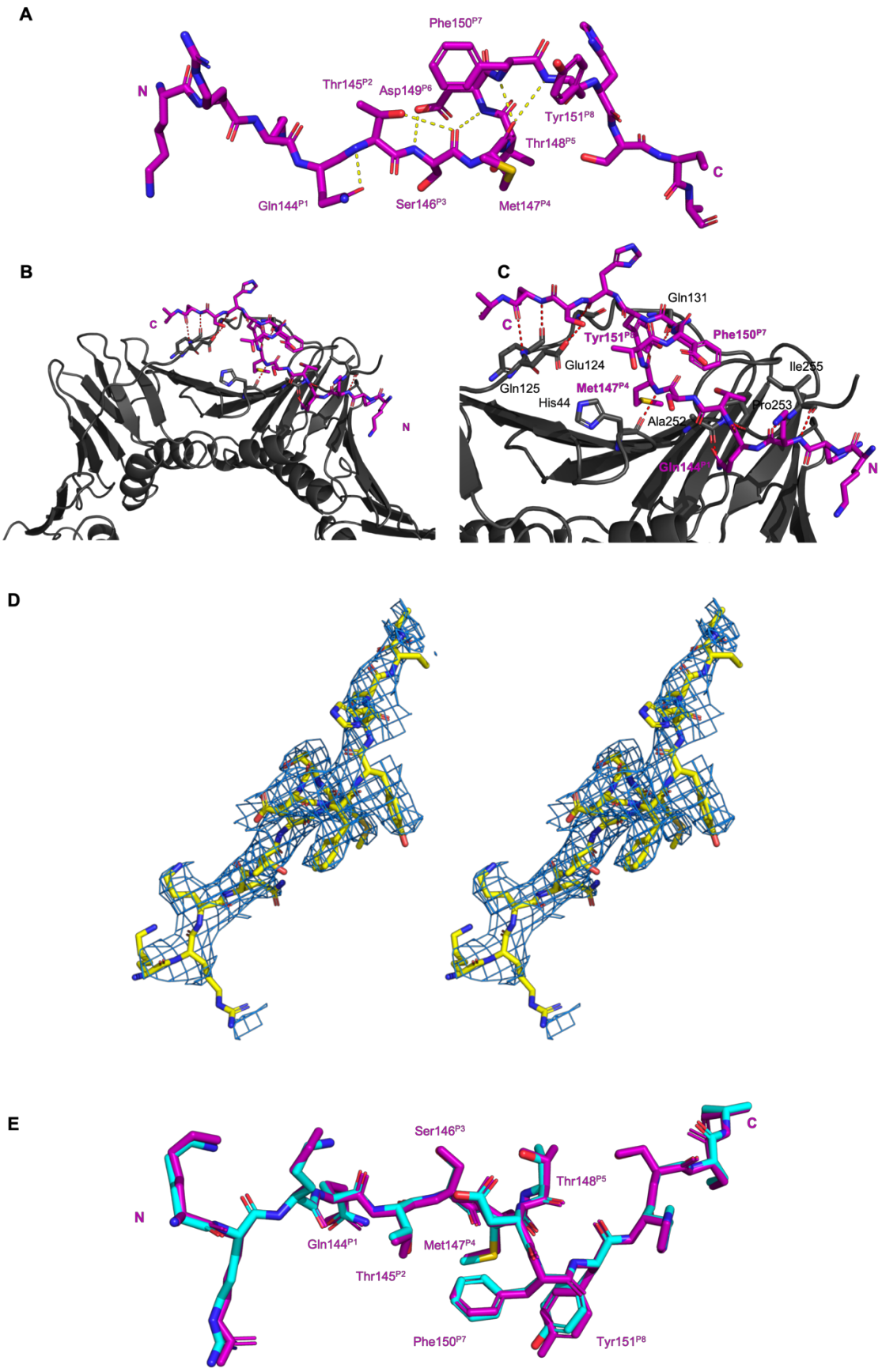

Figure S2: Co-crystal structure of p21$_{\mu}$ (purple, sticks) bound to PCNA monomer (grey, cartoon). Heteroatoms indicated as blue, nitrogen; red, oxygen; yellow, sulfur. **A** Intramolecular interactions shown as yellow dashes, and PIP-box residues labelled in purple. **B** & **C** Intermolecular interactions shown as red dashes, PCNA residues labelled in grey/white and conserved PIP-box residues labelled in purple. **D** Representative electron density of p21$_{\mu}$ (yellow, sticks) shown as a wall-eye stereo image 2Fo-Fc composite omit map, view contoured at 1.5σ. **E** Overlay of p21$_{\mu}$ (purple, sticks) bound to PCNA (not shown) co-crystal structure, with p21$_{\mu}$ (cyan, sticks) that has been energy minimised on the PCNA surface which shows a high degree of structural similarity, and validates the computational modelling approach.

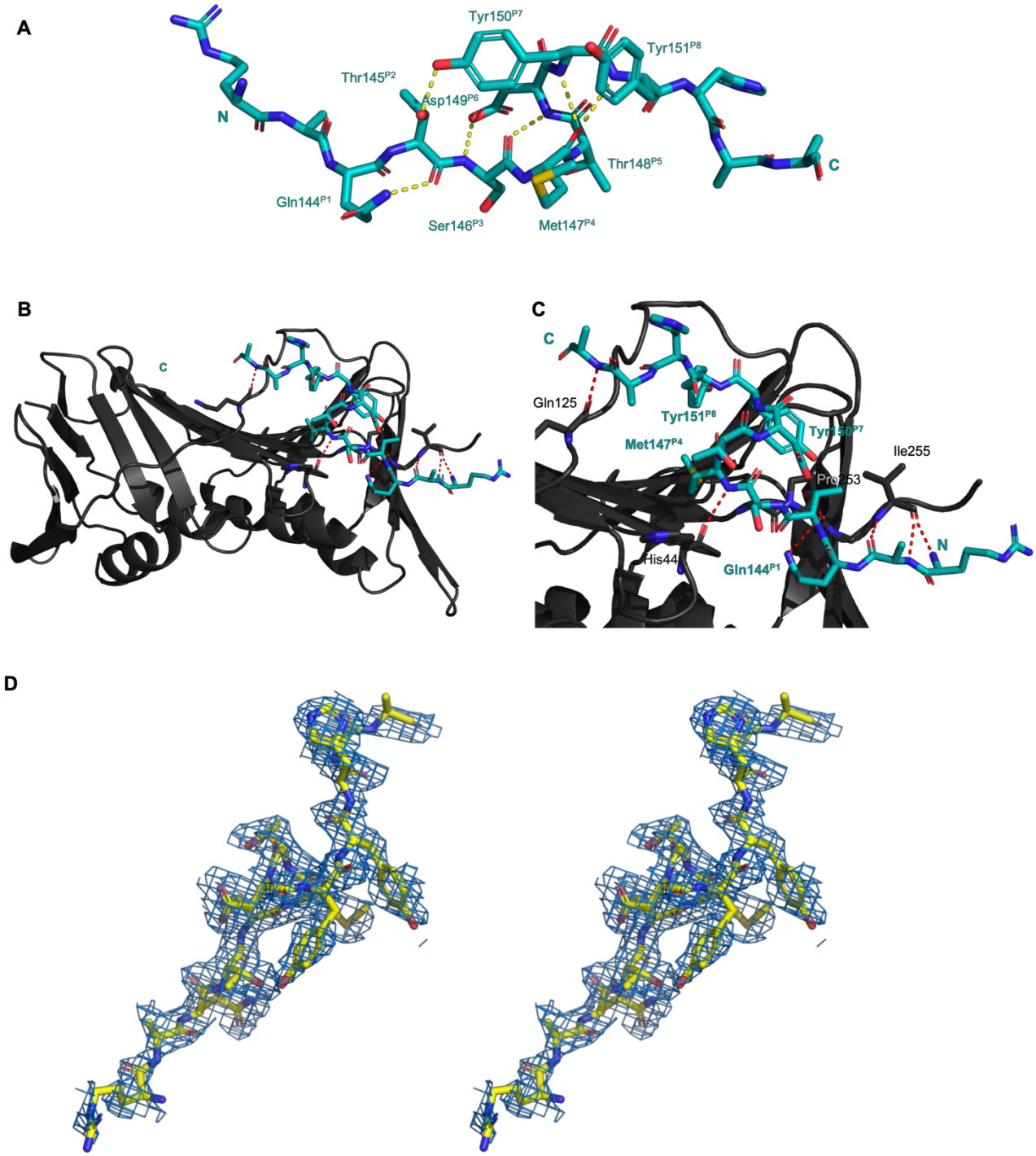

Figure S3: Co-crystal structure of p21$_{\mu}$-F150Y (blue, sticks) bound to PCNA monomer (grey, cartoon). Heteroatoms indicated as blue, nitrogen; red, oxygen; yellow, sulfur **A** Intramolecular interactions shown as yellow dashes, and PIP-box residues labelled in blue. **B** & **C** Intermolecular interactions shown as red dashes, PCNA residues labelled in grey/white and conserved PIP-box residues labelled in blue. **D** Representative electron density of p21$_{\mu}$-F150Y (yellow, sticks) shown as a wall-eye stereo image 2Fo-Fc composite omit map, view contoured at 1.5σ.

COMPUTATIONAL MODELLING OF PCNA MONOMERS BOUND TO P21μ PEPTIDES

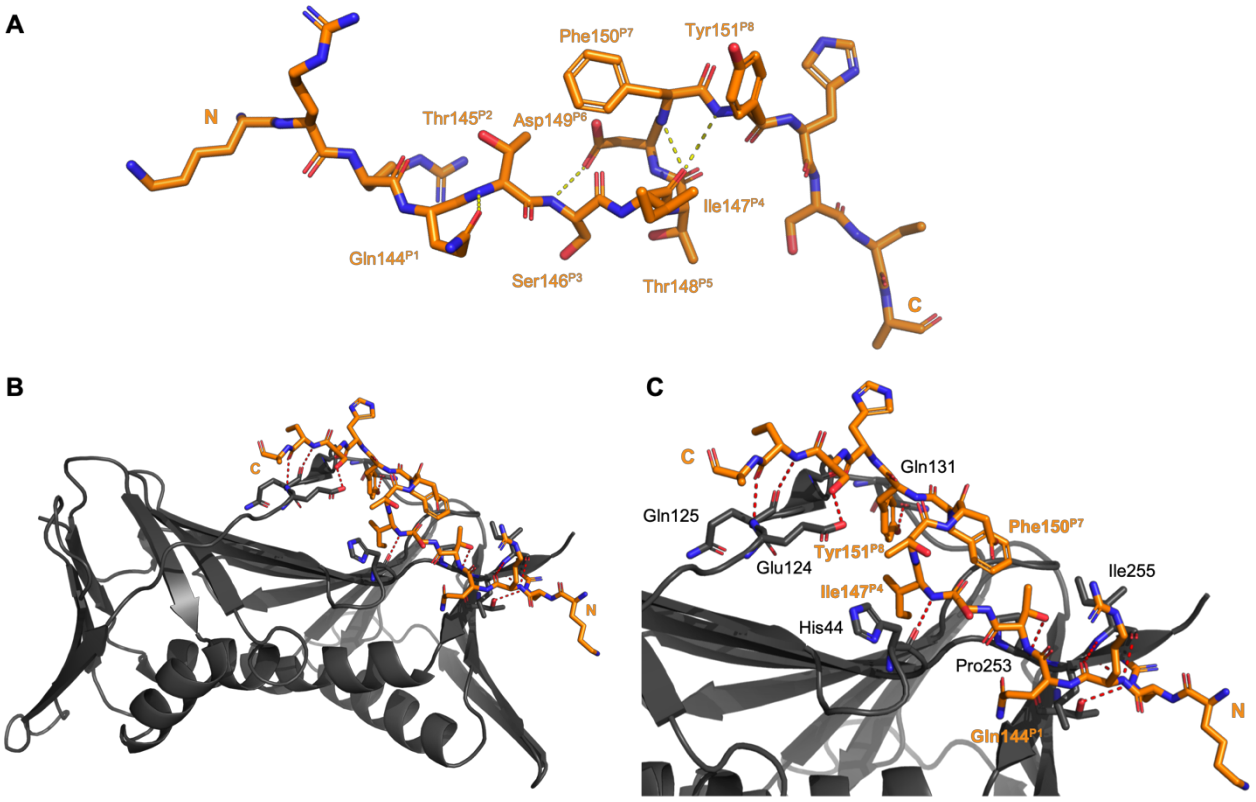

Figure S4: Computationally modelled structure of p21μ-M147I (orange, sticks) on the PIP-box binding site of a hPCNA monomer (grey, cartoon). Heteroatoms indicated as blue, nitrogen; red, oxygen; yellow, sulfur. **A** Intramolecular interactions shown as yellow dashes, and PIP-box residues labelled in orange. **B** & **C** Intermolecular interactions shown as red dashes, PCNA residues labelled in grey/white and conserved PIP-box residues labelled in orange.

Table S6: Secondary Interaction Summary for computationally modelled structured of p21μ-M147I with hPCNA calculated using the RING server. Chain B interactions only. RING Session ID: 5f3b21280e9f94078ea22cfe

		Intermolecular			Intramolecular		
	Residue	**VDW**	**H-Bond**		**VDW**	**H-Bond**	**Total**
FI	141	0	0		0	0	
	142	3	1		0	0	
	143	1	2		0	0	
PIP-box	* **144**	1	0		0	0	
	145	1	1		2	0	
	146	1	0		0	0	
	* **147**	2	1		0	1	
	148	2	0		0	0	
	149	0	0		0	0	
	* **150**	3	0		0	0	
	* **151**	3	2		0	0	
FI	152	0	1		0	0	
	153	1	0		0	0	
	154	1	1		0	0	
	155	0	0		0	0	
	Total	19	9		2	1	31
	PIP-box	13	4		2	1	20
	Flanking (FI)	6	5		0	0	11
	Conserved (*) PIP-box residues	6	1		0	1	8
	Non-conserved PIP-box residues	4	1		2	0	7
	Other: Intermolecular pi-stack between B-Tyr151 and A-Tyr133						

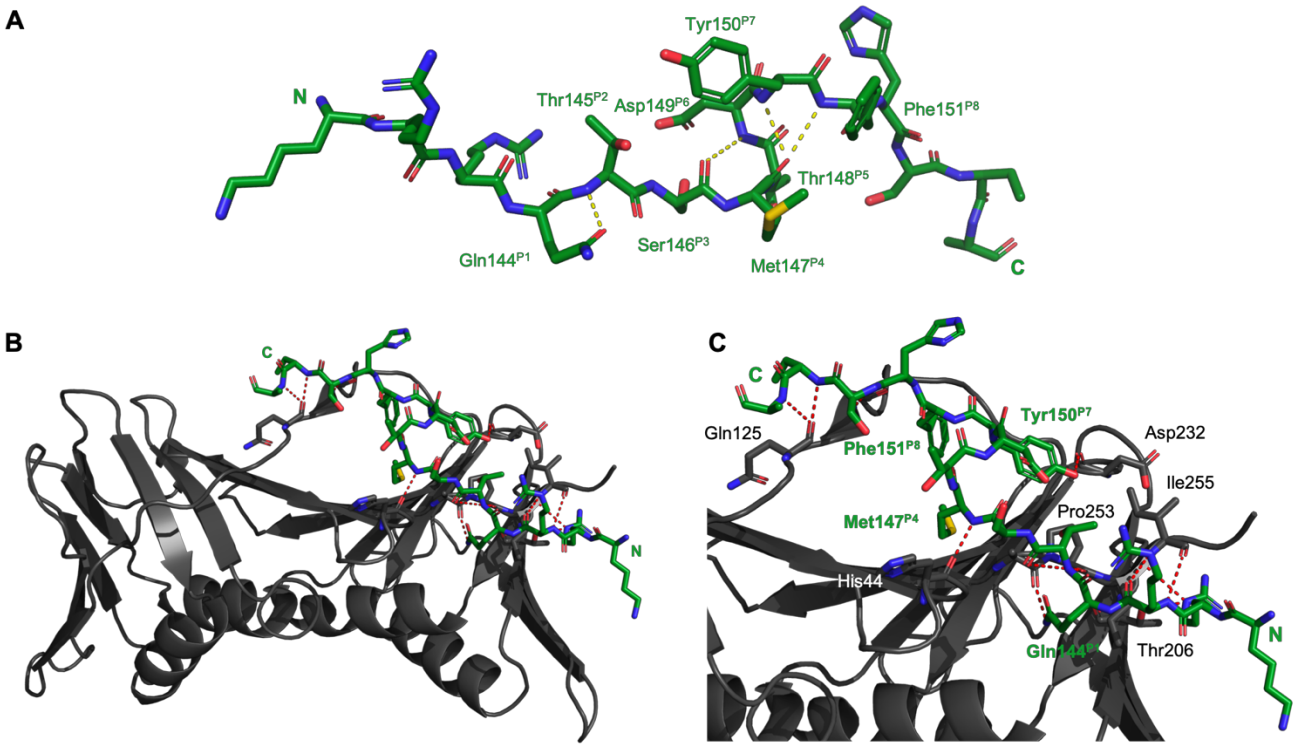

Figure S5: Computationally modelled structure of p21$_{\mu}$- FY150/151YF (dark green, sticks) on the PIP-box binding site of a hPCNA monomer (grey, cartoon). Heteroatoms indicated as blue, nitrogen; red, oxygen; yellow, sulfur. **A** Intramolecular interactions shown as yellow dashes, and PIP-box residues labelled in dark green **B** & **C** Intermolecular interactions shown as red dashes, PCNA residues labelled in grey/white and conserved PIP-box residues labelled in dark green.

Table S7: Secondary Interaction Summary for computationally modelled structured of p21$_{\mu}$-FY150/151YF with hPCNA calculated using the RING server. Chain B interactions only. RING session ID: 5f3b22bc0e9f94078ea22d03

		Intermolecular			Intramolecular		
	Residue	**VDW**	**H-Bond**		**VDW**	**H-Bond**	**Total**
FI	141	0	0		0	0	
	142	4	2		0	0	
	143	1	1		0	0	
PIP-box	* **144**	2	0		0	0	
	145	1	1		0	0	
	146	1	0		0	1	
	* **147**	6	1		1	2	
	148	1	0		0	0	
	149	0	0		0	0	
	* **150**	3	1		0	0	
	* **151**	2	0		0	0	
FI	152	0	0		0	0	
	153	1	0		0	0	
	154	2	1		0	0	
	155	0	1		0	0	
	Total	24	8		1	3	36
	PIP-box	16	3		1	3	23
	Flanking (FI)	8	5		0	0	13
	Conserved (*) PIP-box residues	11	2		1	2	16
	Non-conserved PIP-box residues	3	1		0	1	5
	Other: Intermolecular ionic interaction between B-Arg143 and A-Asp257; Intermolecular pi-stack between B-Tyr151 and A-Tyr250						

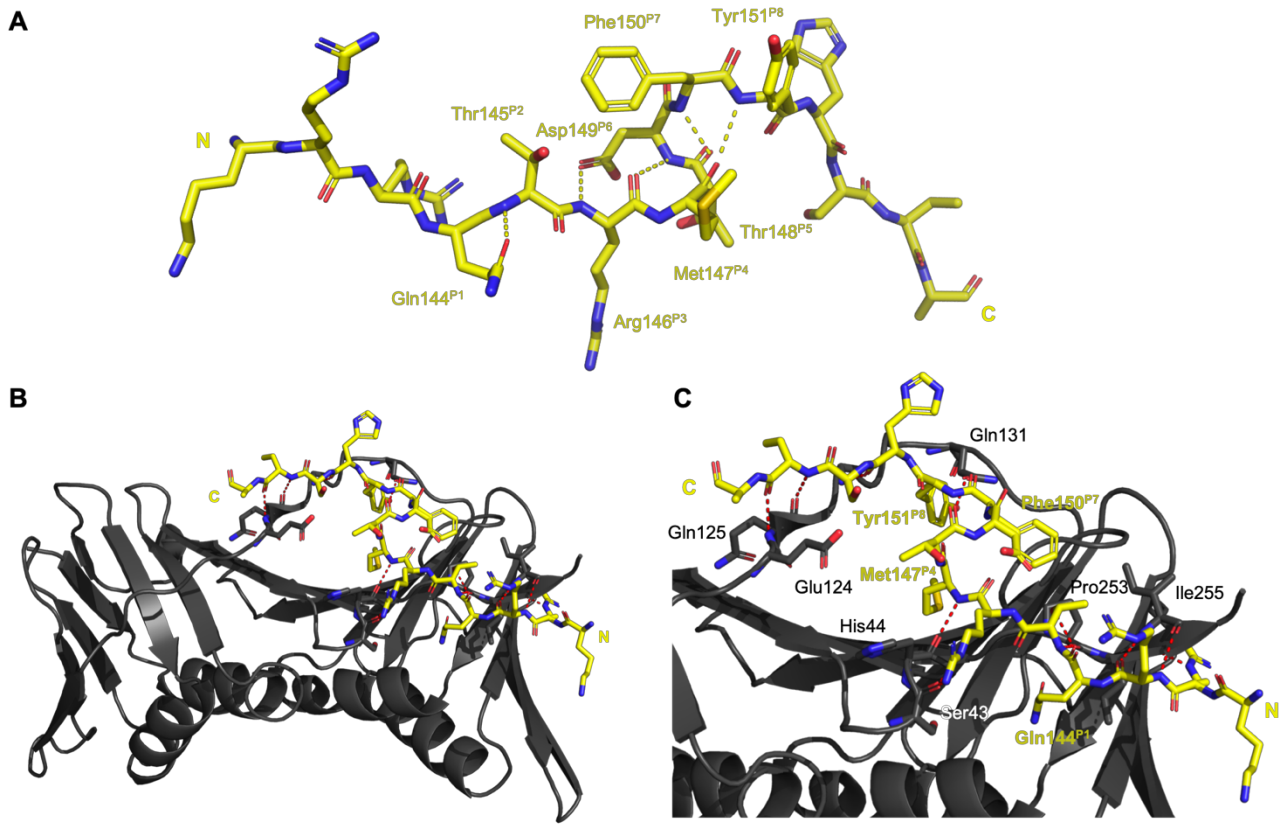

Figure S6: Computationally modelled structure of p21$_{\mu}$-S146R (yellow, sticks) on the PIP-box binding site of a hPCNA monomer (grey, cartoon). Heteroatoms indicated as blue, nitrogen; red, oxygen; yellow, sulfur. **A** Intramolecular interactions shown as yellow dashes, and PIP-box residues labelled in yellow. **B** & **C** Intermolecular interactions shown as red dashes, PCNA residues labelled in grey/white and conserved PIP-box residues labelled in yellow.

Table S8: Secondary Interaction Summary for computationally modelled structured of p21$_{\mu}$-S146R with hPCNA calculated using the RING server. Chain B interactions only. RING Session ID: [5f3b1f6b0e9f94078ea22cf9]

		Intermolecular			Intramolecular		
	Residue	**VDW**	**H-Bond**		**VDW**	**H-Bond**	**Total**
Fl	141	0	0		0	0	
	142	3	1		0	0	
	143	2	2		0	0	
PIP-box	* **144**	1	0		0	0	
	145	1	1		1	0	
	146	2	1		0	1	
	* **147**	4	1		1	2	
	148	0	0		0	0	
	149	0	0		0	0	
	* **150**	3	0		0	0	
	* **151**	2	1		0	0	
Fl	152	0	1		0	0	
	153	2	0		0	0	
	154	0	1		0	0	
	155	0	1		0	0	
	Total	20	10		2	3	35
	PIP-box	13	4		2	3	22
	Flanking (Fl)	7	6		0	0	13
	Conserved (*) PIP-box residues	8	1		1	2	12
	Non-conserved PIP-box residues	3	2		1	1	7
	Other: Intermolecular ionic interaction between B-Arg143 and A-Asp257						

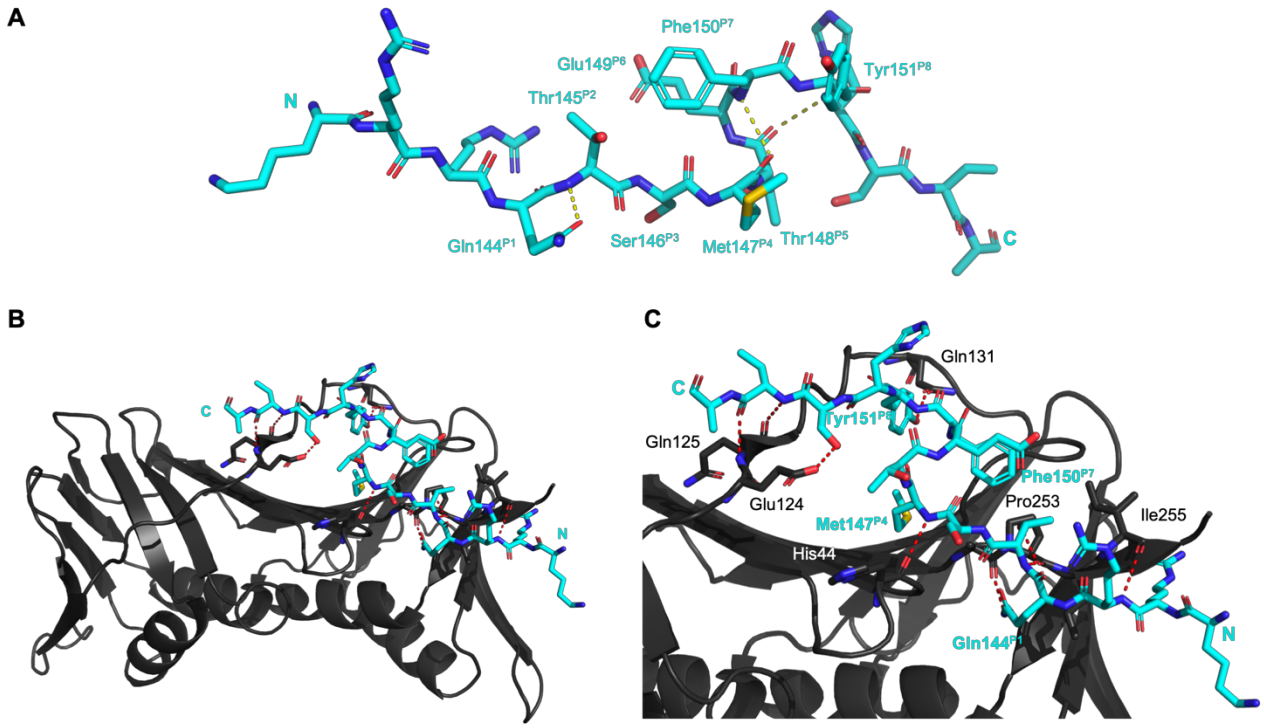

Figure S7: Computationally modelled structure of p21$_{\mu}$- D149E (light blue, sticks) on the PIP-box binding site of a hPCNA monomer (grey, cartoon). Heteroatoms indicated as blue, nitrogen; red, oxygen; yellow, sulfur. **A** Intramolecular interactions shown as yellow dashes, and PIP-box residues labelled in light blue. **B** & **C** Intermolecular interactions shown as red dashes, PCNA residues labelled in grey/white and conserved PIP-box residues labelled in light blue.

Table S9: Secondary Interaction Summary for computationally modelled structured of p21$_{\mu}$-D149E with hPCNA calculated using the RING server. Chain B interactions only. RING Session ID: 5f3b21fe0e9f94078ea22d00

		Intermolecular			Intramolecular		
	Residue	**VDW**	**H-Bond**		**VDW**	**H-Bond**	**Total**
Fl	141	0	0		0	0	
	142	2	2		0	0	
	143	0	2		0	0	
PIP-box	* **144**	2	0		0	0	
	145	1	1		1	0	
	146	1	0		0	1	
	* **147**	4	1		1	2	
	148	1	0		0	0	
	149	0	0		1	0	
	* **150**	3	0		0	0	
	* **151**	4	2		0	0	
Fl	152	1	0		0	0	
	153	1	0		0	0	
	154	0	1		0	0	
	155	0	0		0	0	
	Total	20	9		3	3	35
	PIP-box	16	4		3	3	26
	Flanking (Fl)	4	5		0	0	9
	Conserved (*) PIP-box residues	9	1		2	2	14
	Non-conserved PIP-box residues	3	1		2	1	7
	Other: Intermolecular ionic interaction between B-Arg143 and A-Asp257; Intermolecular pi-stack between B-Tyr151 and A-Tyr250						

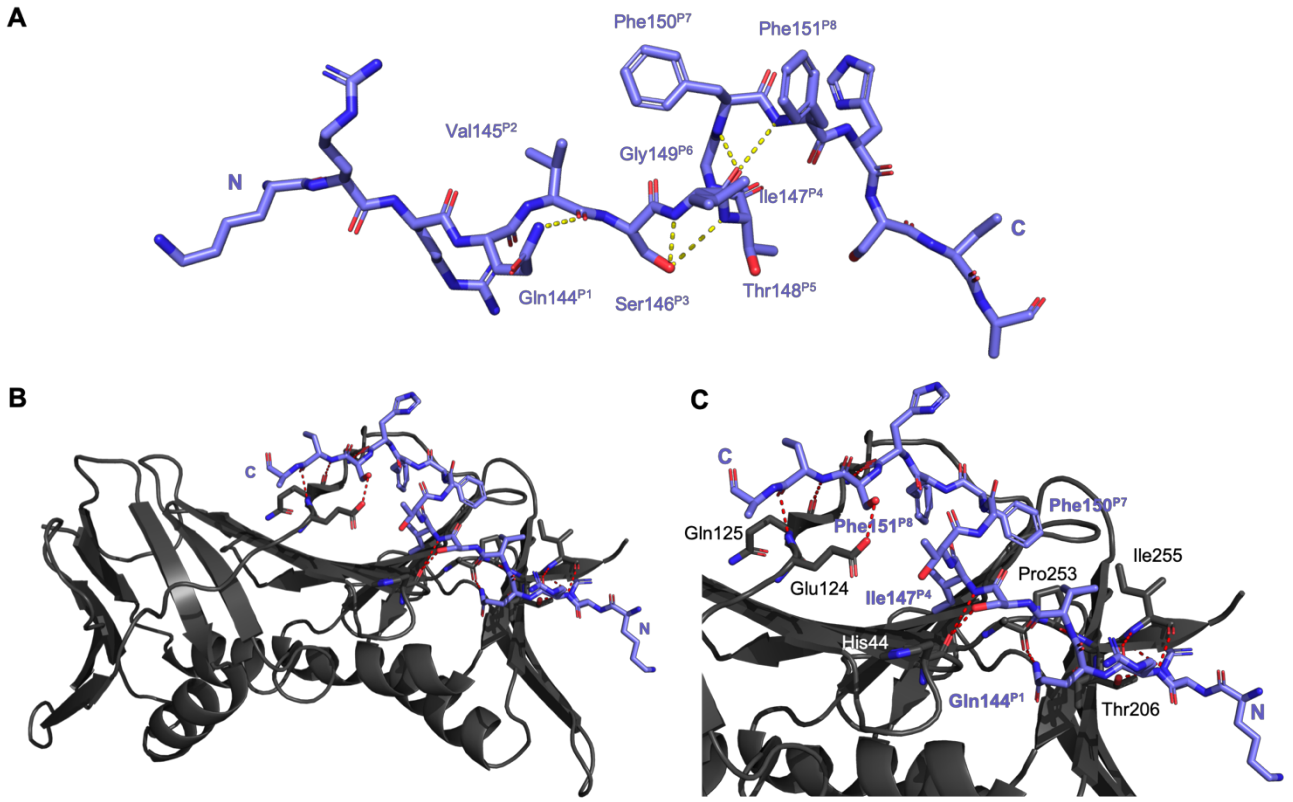

Figure S8: Computationally modelled structure of p21$_{\mu}$- pol δ_{p66} (light purple, sticks) on the PIP-box binding site of a hPCNA monomer (grey, cartoon). Heteroatoms indicated as blue, nitrogen; red, oxygen; yellow, sulfur. **A** Intramolecular interactions shown as yellow dashes, and PIP-box residues labelled in light purple. **B** & **C** Intermolecular interactions shown as red dashes, PCNA residues labelled in grey/white and conserved PIP-box residues labelled in light purple.

Table S10: Secondary Interaction Summary for computationally modelled structured of p21$_{\mu}$-pol δ_{p66} with hPCNA calculated using the RING server. Chain B interactions only. RING Session ID: 5f3b202a0e9f94078ea22cfb

		Intermolecular			Intramolecular		
	Residue	**VDW**	**H-Bond**		**VDW**	**H-Bond**	**Total**
FI	141	0	0		0	0	
	142	3	2		0	0	
	143	1	2		0	0	
PIP-box	* **144**	2	0		0	0	
	145	1	1		1	0	
	146	0	0		0	0	
	* **147**	5	0		1	2	
	148	0	0		0	0	
	149	0	0		0	0	
	* **150**	1	0		0	0	
	* **151**	2	0		0	0	
FI	152	0	1		0	0	
	153	2	0		0	0	
	154	0	1		0	0	
	155	1	0		0	0	
	Total	18	7		2	2	29
	PIP-box	11	1		2	2	16
	Flanking (FI)	7	6		0	0	13
	Conserved (*) PIP-box residues	8	0		1	2	11
	Non-conserved PIP-box residues	1	1		1	0	3
	Other: Intermolecular pi-stack between B-Phe151 and A-Tyr250						

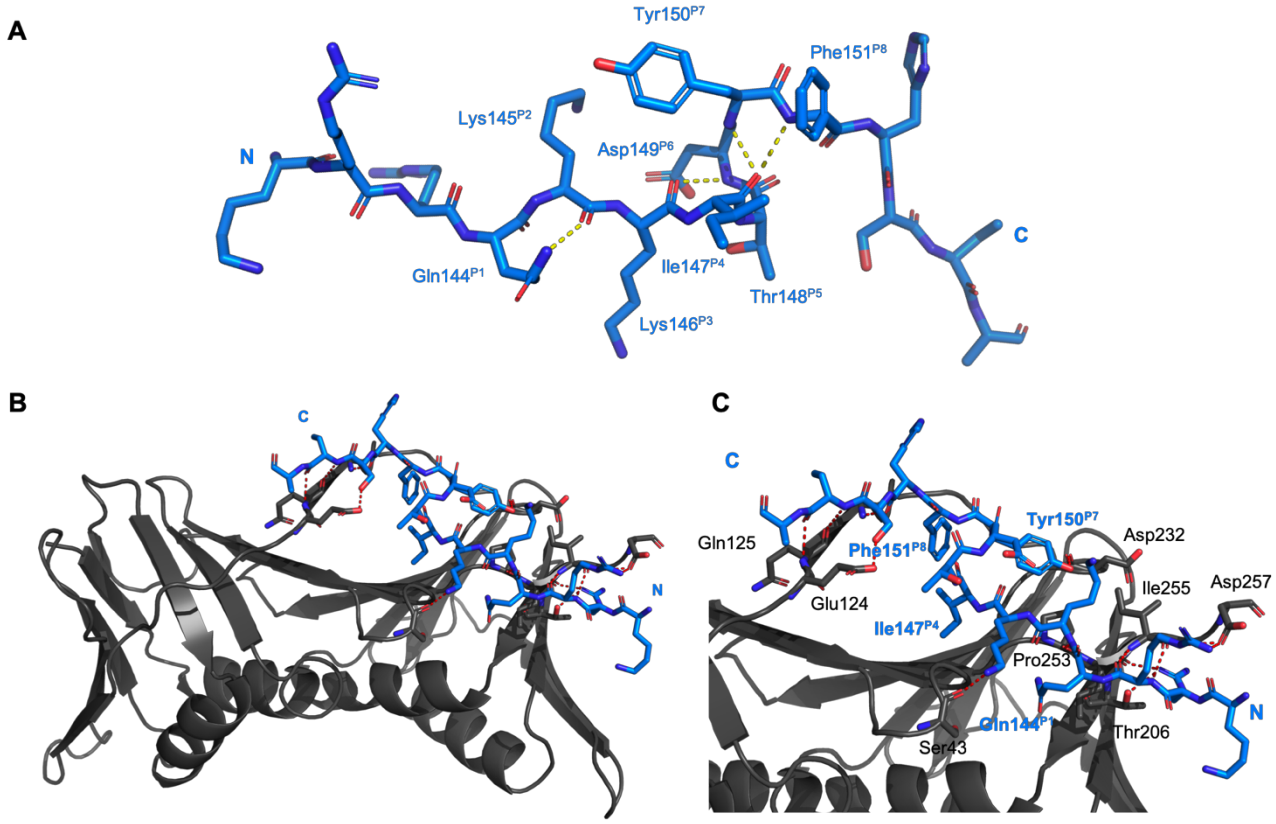

Figure S9: Computationally modelled structure of p21$_{\mu}$-Pogo (dark blue, sticks) on the PIP-box binding site of a hPCNA monomer (grey, cartoon). Heteroatoms indicated as blue, nitrogen; red, oxygen; yellow, sulfur. **A** Intramolecular interactions shown as yellow dashes, and PIP-box residues labelled in blue. **B** & **C** Intermolecular interactions shown as red dashes, PCNA residues labelled in grey/white and conserved PIP-box residues labelled in blue.

Table S11: Secondary Interaction Summary for computationally modelled structured of p21$_{\mu}$-Pogo with hPCNA calculated using the RING server. Chain B interactions only. RING Session ID: 5f3b224d0e9f94078ea22d01

		Intermolecular			Intramolecular		
	Residue	**VDW**	**H-Bond**		**VDW**	**H-Bond**	**Total**
FI	141	0	0		0	0	
	142	3	2		0	0	
	143	1	2		0	0	
PIP-box	* **144**	2	0		0	0	
	145	2	0		0	0	
	146	1	0		0	1	
	* **147**	7	0		1	2	
	148	1	0		0	0	
	149	0	0		0	0	
	* **150**	3	1		0	0	
	* **151**	3	0		0	0	
FI	152	0	1		0	0	
	153	0	0		0	0	
	154	0	1		0	0	
	155	0	0		0	0	
	Total	23	7		1	3	34
	PIP-box	19	1		1	3	24
	Flanking (FI)	4	6		0	0	10
	Conserved (*) PIP-box residues	12	1		1	2	16
	Non-conserved PIP-box residues	4	0		0	1	5
	Other: Intermolecular ionic interaction between B-Arg143 and A-Asp257; Intermolecular pi-stack between B-Phe151 and A-Tyr250						

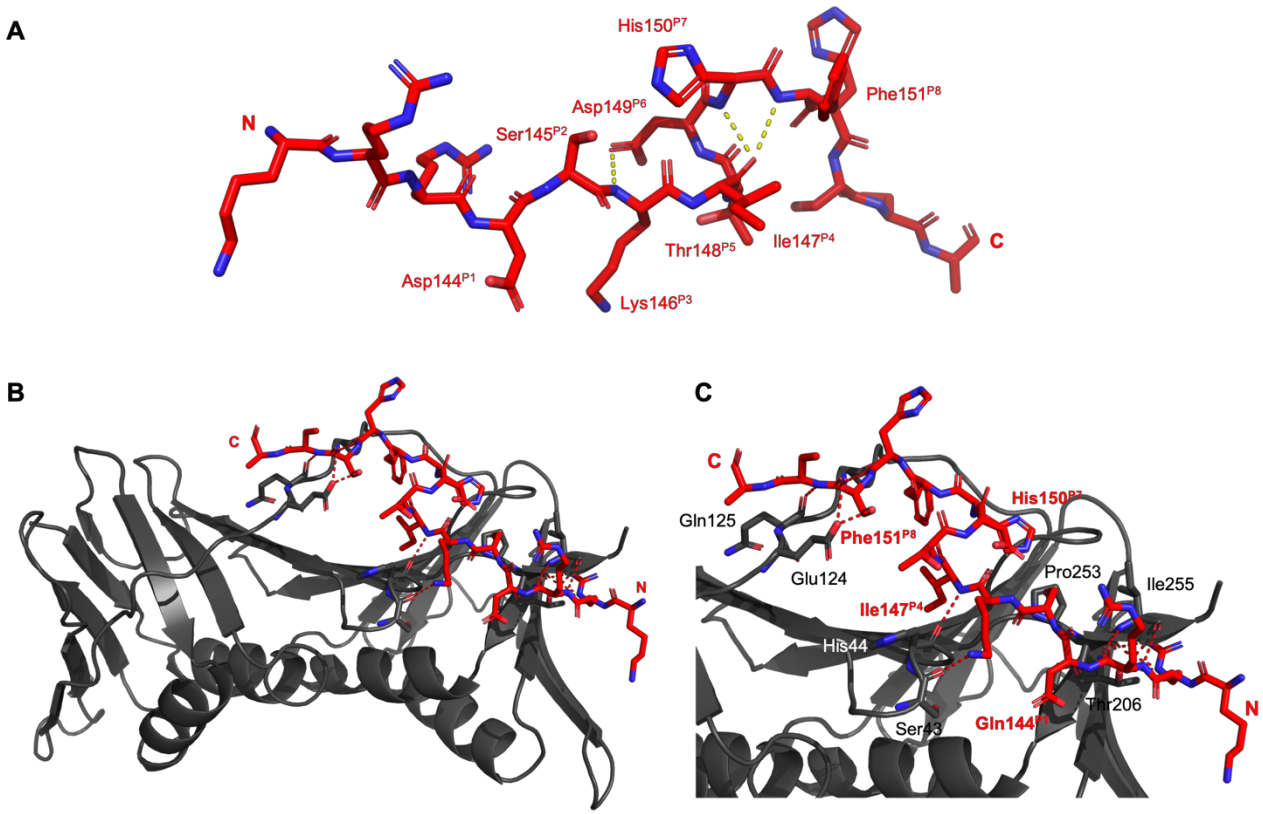

Figure S10: Computationally modelled structure of p21$_{\mu}$- PARG (red, sticks) on the PIP-box binding site of a hPCNA monomer (grey, cartoon). Heteroatoms indicated as blue, nitrogen; red, oxygen; yellow, sulfur. **A** Intramolecular interactions shown as yellow dashes, and PIP-box residues labelled in red. **B** & **C** Intermolecular interactions shown as red dashes, PCNA residues labelled in grey/white and conserved PIP-box residues labelled in red.

Table S12: Secondary Interaction Summary for computationally modelled structured of p21$_{\mu}$-PARG with hPCNA calculated using the RING server. Chain B interactions only. RING Session ID: 5f3b1de50e9f94078ea22cf7

		Intermolecular			Intramolecular		
	Residue	**VDW**	**H-Bond**		**VDW**	**H-Bond**	**Total**
FI	141	0	0		0	0	
	142	2	2		0	0	
	143	0	2		0	0	
PIP-box	* **144**	1	0		0	0	
	145	1	0		0	0	
	146	1	0		0	1	
	* **147**	2	1		0	2	
	148	0	0		0	0	
	149	0	0		0	0	
	* **150**	3	0		0	0	
	* **151**	3	0		0	0	
FI	152	0	1		0	0	
	153	1	0		0	0	
	154	0	1		0	0	
	155	0	0		0	0	
	Total	14	7		0	3	24
	PIP-box	11	1		0	3	15
	Flanking (FI)	3	6		0	0	9
	Conserved (*) PIP-box residues	5	1		0	2	8
	Non-conserved PIP-box residues	3	0		0	1	4
	Other: Intermolecular pi-stack between B-Tyr151 and A-Tyr250						

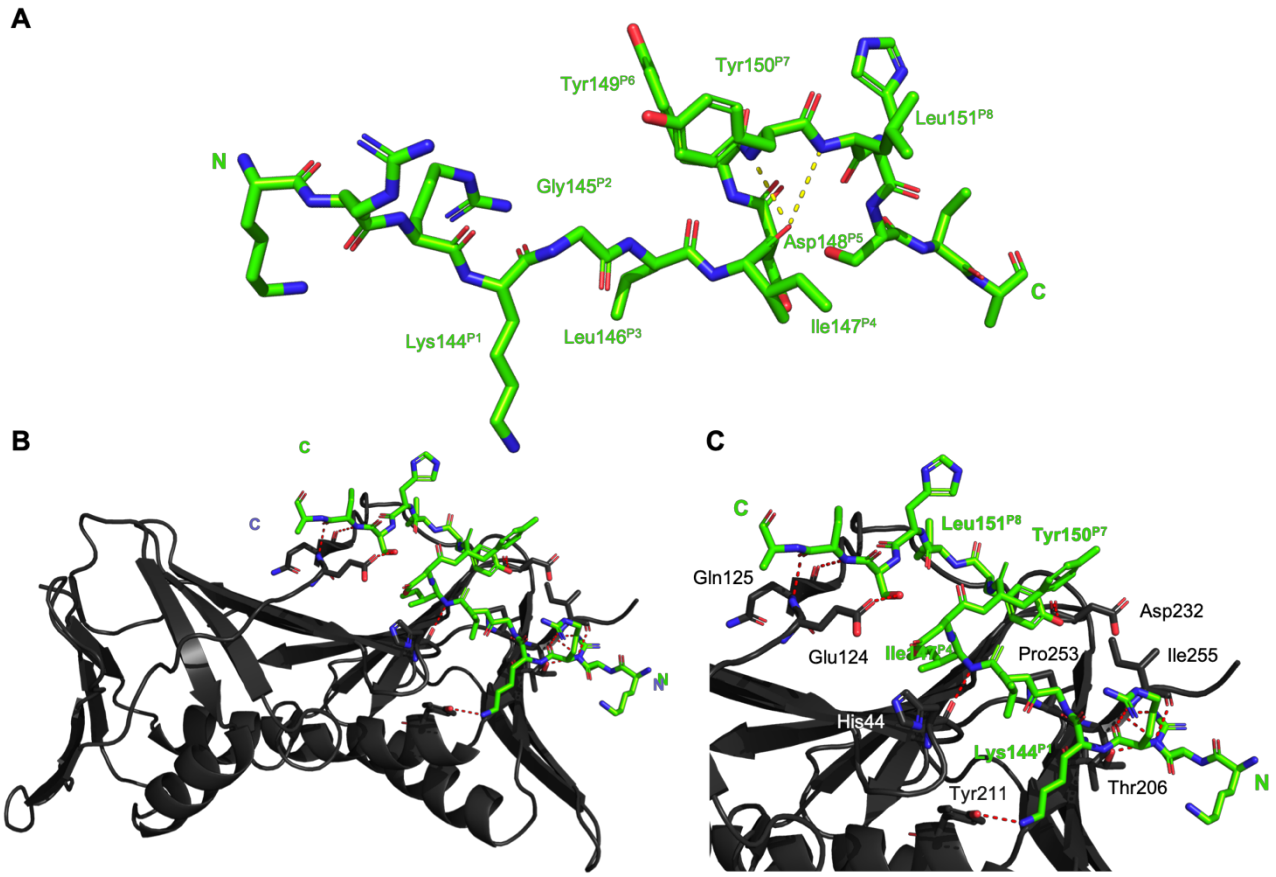

Figure S11: Computationally modelled structure of p21$_{\mu}$-pol ι (green, sticks) on the PIP-box binding site of a hPCNA monomer (grey, cartoon). Heteroatoms indicated as blue, nitrogen; red, oxygen; yellow, sulfur. **A** Intramolecular interactions shown as yellow dashes, and PIP-box residues labelled in green **B** & **C** Intermolecular interactions shown as red dashes, PCNA residues labelled in grey/white and conserved PIP-box residues labelled in green

Table S13: Secondary Interaction Summary for computationally modelled structured of p21$_{\mu}$-pol ι with hPCNA calculated using the RING server. Chain B interactions only. RING Session ID: 5f3b1e580e9f94078ea22cf8

		Intermolecular			Intramolecular		
	Residue	**VDW**	**H-Bond**		**VDW**	**H-Bond**	**Total**
FI	141	0	0		0	0	
	142	2	2		0	0	
	143	0	2		0	0	
PIP-box	* **144**	1	0		0	0	
	145	1	1		0	0	
	146	2	0		1	0	
	* **147**	3	1		0	1	
	148	1	0		0	0	
	149	0	0		0	0	
	* **150**	2	1		0	0	
	* **151**	1	0		0	0	
FI	152	0	1		0	0	
	153	2	0		0	0	
	154	0	1		0	0	
	155	0	0		0	0	
	Total	15	9		1	1	26
	PIP-box	11	3		1	1	16
	Flanking (FI)	4	6		0	0	10
	Conserved (*) PIP-box residues	6	2		0	1	9
	Non-conserved PIP-box residues	5	1		1	0	7
	Other:						

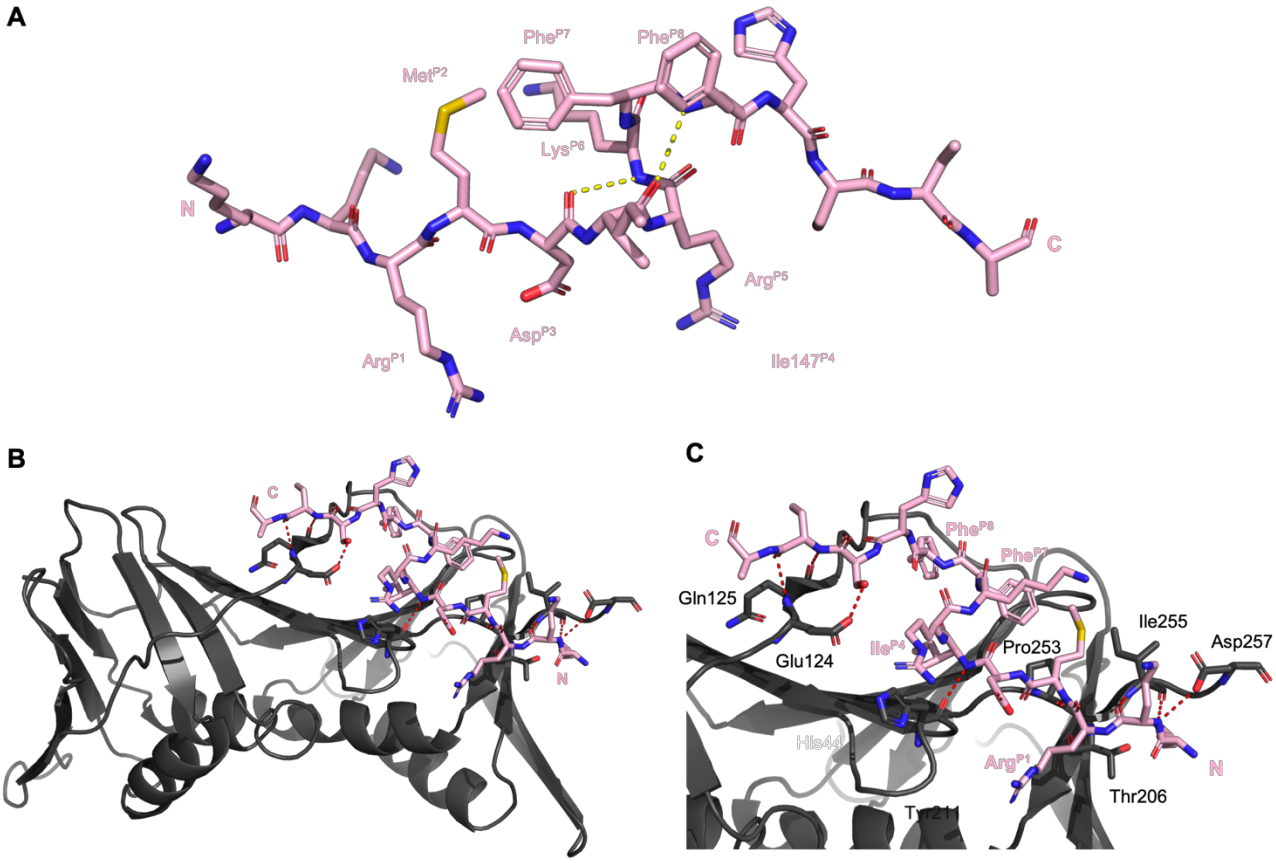

Figure S12: Computationally modelled structure of p21$_{\mu}$-RFC (light pink, sticks) on the PIP-box binding site of a hPCNA monomer (grey, cartoon). Heteroatoms indicated as blue, nitrogen; red, oxygen; yellow, sulfur. **A** Intramolecular interactions shown as yellow dashes, and PIP-box residues labelled in light pink **B** & **C** Intermolecular interactions shown as red dashes, PCNA residues labelled in grey/white and conserved PIP-box residues labelled in light pink

Table S14: Secondary Interaction Summary for computationally modelled structured of p21$_{\mu}$-RFC with hPCNA calculated using the RING server. Chain B interactions only. RING Session ID: 5f3b20890e9f94078ea22cfd

		Intermolecular			Intramolecular		
	Residue	**VDW**	**H-Bond**		**VDW**	**H-Bond**	**Total**
FI	142	3	0		0	0	
	143	1	2		0	0	
PIP-box	**144**	1	0		0	0	
	145	2	1		1	0	
	146	1	0		0	2	
	* **147**	2	1		0	2	
	148	1	0		0	0	
	149	0	0		0	0	
	* **150**	2	0		0	0	
	* **151**	2	0		0	0	
FI	152	0	0		0	0	
	153	2	0		0	0	
	154	0	1		0	0	
	155	0	0		0	0	
	Total	17	5		1	4	27
	PIP-box	11	2		1	4	18
	Flanking (FI)	6	3		0	0	9
	Conserved (*) PIP-box residues	6	1	0	0	2	9
	Non-conserved PIP-box residues	5	1	0	1	2	9
	Other: Intermolecular ionic interaction between B-Arg143 and A-Asp257; Intermolecular pi-stack between B-Tyr151 and A-Tyr250						

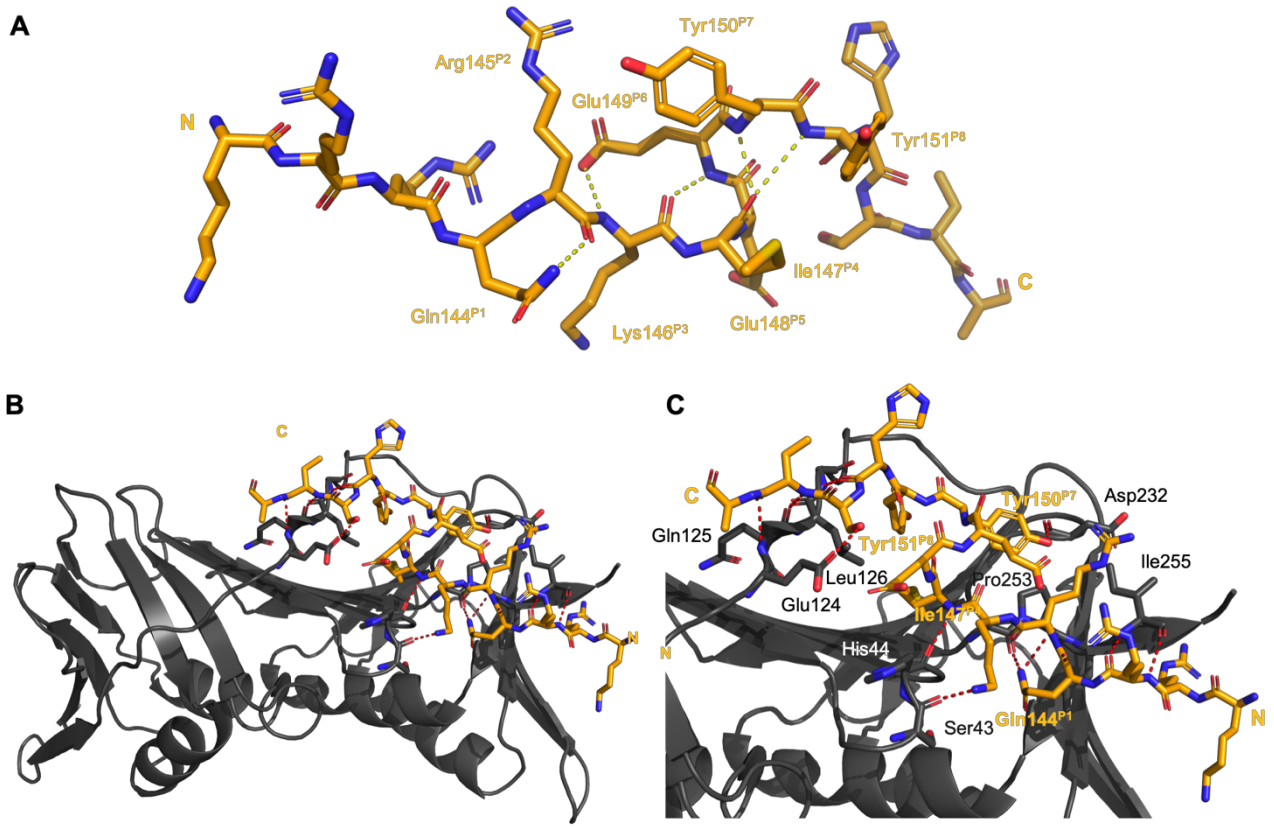

Figure S13: Computationally modelled structure of p21$_{\mu}$-RD1 (light orange, sticks) on the PIP-box binding site of a hPCNA monomer (grey, cartoon). Heteroatoms indicated as blue, nitrogen; red, oxygen; yellow, sulfur. **A** Intramolecular interactions shown as yellow dashes, and PIP-box residues labelled in light orange. **B** & **C** Intermolecular interactions shown as red dashes, PCNA residues labelled in grey/white and conserved PIP-box residues labelled in light orange.

Table S15: Secondary Interaction Summary for computationally modelled structured of p21$_{\mu}$-RD1 with hPCNA calculated using the RING server. Chain B interactions only. RING Session ID: 5f3b21c10e9f94078ea22cff

		Intermolecular			Intramolecular		
	Residue	**VDW**	**H-Bond**		**VDW**	**H-Bond**	**Total**
FI	141	0	0		0	0	
	142	3	2		0	0	
	143	1	1		0	0	
PIP-box	* **144**	2	0		0	0	
	145	1	1		1	0	
	146	0	0		0	1	
	* **147**	4	1		1	2	
	148	1	0		0	0	
	149	0	0		0	0	
	* **150**	3	1		0	0	
	* **151**	3	0		0	0	
FI	152	0	1		0	0	
	153	1	0		0	0	
	154	0	1		0	0	
	155	0	0		0	0	
	Total	19	8		2	3	32
	PIP-box	14	3		2	3	22
	Flanking (FI)	5	5		0	0	10
	Conserved (*) PIP-box residues	9	2		1	2	14
	Non-conserved PIP-box residues	2	1		1	1	5
	Other: Intermolecular ionic interaction between B-Arg143 and A-Asp257; Intermolecular pi-stack between B-Tyr151 and A-Tyr250						

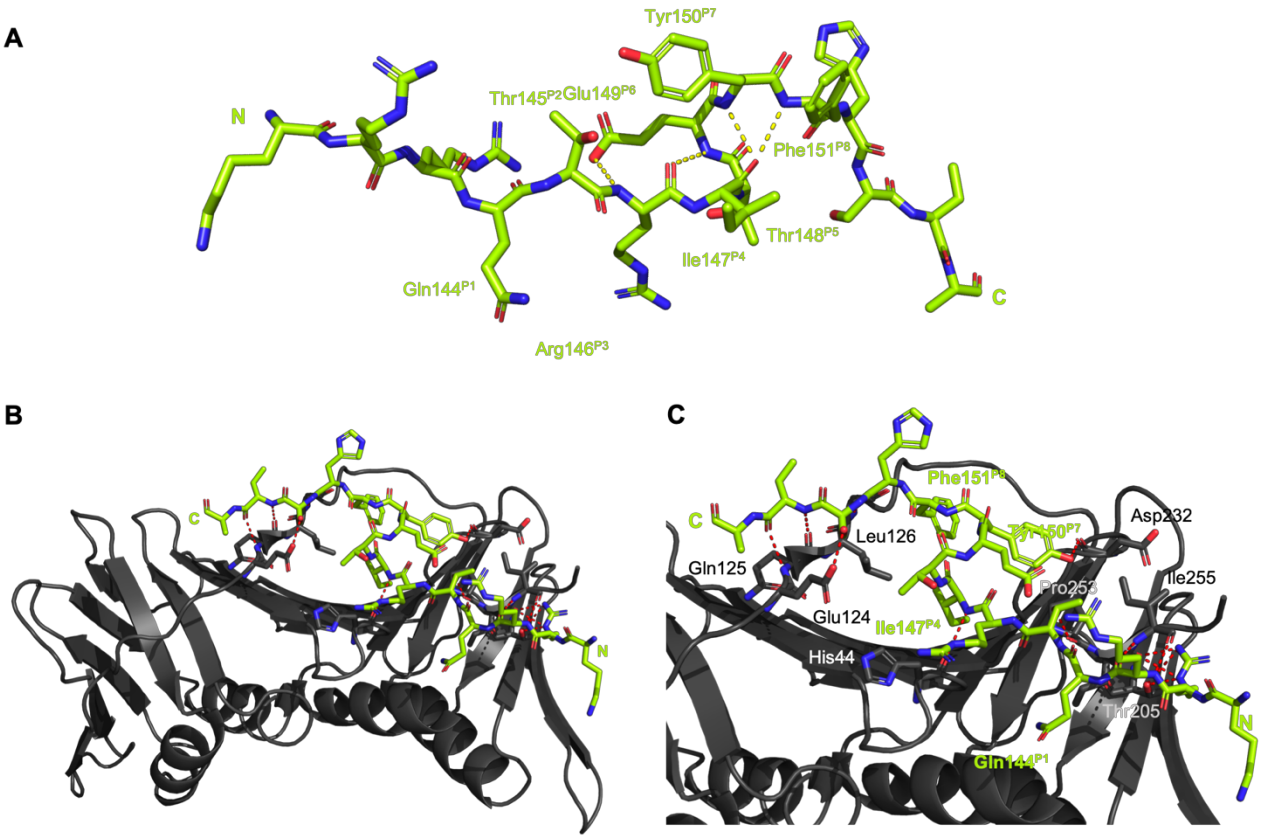

Figure S14: Computationally modelled structure of p21$_{\mu}$-RD2 (green, sticks) on the PIP-box binding site of a hPCNA monomer (grey, cartoon). Heteroatoms indicated as blue, nitrogen; red, oxygen; yellow, sulfur. **A** Intramolecular interactions shown as yellow dashes, and PIP-box residues labelled in green. **B** & **C** Intermolecular interactions shown as red dashes, PCNA residues labelled in grey/white and conserved PIP-box residues labelled in green.

Table S16: Secondary Interaction Summary for computationally modelled structured of p21$_{\mu}$-RD2 with hPCNA calculated using the RING server. Chain B interactions only. RING Session ID: 5f3b1ff30e9f94078ea22cfa

		Intermolecular			Intramolecular		
	Residue	**VDW**	**H-Bond**		**VDW**	**H-Bond**	**Total**
FI	141	0	0		0	0	
	142	2	2		0	0	
	143	0	1		0	0	
PIP-box	* **144**	1	0		0	0	
	145	1	1		0	0	
	146	2	1		0	1	
	* **147**	7	1		1	2	
	148	1	0		0	0	
	149	0	0		0	0	
	* **150**	2	1		0	0	
	* **151**	2	0		0	0	
FI	152	0	0		0	0	
	153	0	0		0	0	
	154	2	1		0	0	
	155	0	1		0	0	
	Total	20	9		1	3	33
	PIP-box	16	4		1	3	24
	Flanking (FI)	4	5		0	0	9
	Conserved (*) PIP-box residues	10	2		1	2	15
	Non-conserved PIP-box residues	4	2		0	1	7
	Other:						

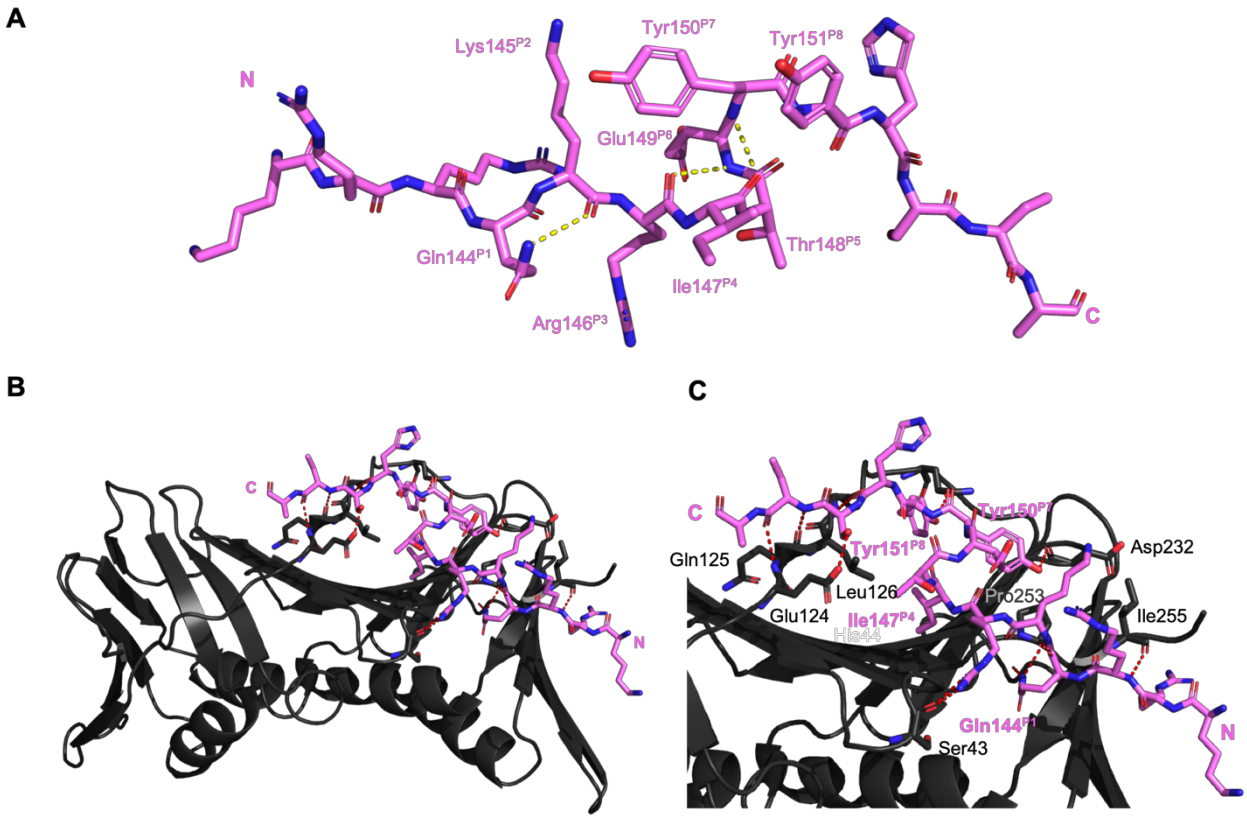

Figure S15: Computationally modelled structure of p21$_{\mu}$-RD3 (pink, sticks) on the PIP-box binding site of a hPCNA monomer (grey, cartoon). Heteroatoms indicated as blue, nitrogen; red, oxygen; yellow, sulfur. **A** Intramolecular interactions shown as yellow dashes, and PIP-box residues labelled in pink. **B** & **C** Intermolecular interactions shown as red dashes, PCNA residues labelled in grey/white and conserved PIP-box residues labelled in pink.

Table S17: Secondary Interaction Summary for computationally modelled structured of p21$_{\mu}$-RD3 with hPCNA calculated using the RING server. Chain B interactions only. RING Session ID: 5f3b22e70e9f94078ea22d04

		Intermolecular			Intramolecular		
	Residue	**VDW**	**H-Bond**		**VDW**	**H-Bond**	**Total**
FI	141	0	0		0	0	
	142	2	1		0	0	
	143	2	2		0	0	
PIP-box	* **144**	1	0		0	0	
	145	0	0		2	0	
	146	2	1		0	1	
	* **147**	5	0		0	2	
	148	1	0		0	0	
	149	0	0		0	0	
	* **150**	2	1		0	0	
	* **151**	2	1		0	0	
FI	152	0	1		0	0	
	153	2	0		0	0	
	154	0	1		0	0	
	155	0	0		0	0	
	Total	19	8		2	3	32
	PIP-box	13	3		2	3	21
	Flanking (FI)	6	5		0	0	11
	Conserved (*) PIP-box residues	8	1		0	2	11
	Non-conserved PIP-box residues	3	1		2	1	7
	Other:						

ANALYSIS OF STRUCTURES

Table S18: Root-mean-squared deviation (RMSD) values of mutant peptides docked to the monomer of hPCNA compared to structures of $p21_{\mu}$ bound to hPCNA and p21 bound to hPCNA.

Name	Structure Type	RMSD value against Wild Type $p21_{139-160}$ (monomer of 1AXC)	RMSD value against monomer of $p21_{\mu}$ bound to hPCNA (PDB ID: 7KQ1)
$p21_{\mu}$	Co-crystal – 7KQ1	0.511	-
$p21_{\mu}$	Computational model	0.316	0.233
$p21_{\mu}$-F150Y	Co-crystal – 7KQ0	0.342	0.451
$p21_{\mu}$-S146R	Computational model	0.570	0.176
$p21_{\mu}$-M147I	Computational model	0.571	0.191
$p21_{\mu}$-D149E	Computational model	0.556	0.197
$p21_{\mu}$-FY150/151YF	Computational model	0.559	0.183
$p21_{\mu}$-PARG	Computational model	0.571	0.192
$p21_{\mu}$-Pogo	Computational model	0.554	0.271
$p21_{\mu}$-pol δ_{p66}	Computational model	0.559	0.186
$p21_{\mu}$-pol ι	Computational model	0.563	0.199
$p21_{\mu}$-RFC	Computational model	0.567	0.209
$p21_{\mu}$-RD1	Computational model	0.600	0.270
$p21_{\mu}$-RD2	Computational model	0.558	0.181
$p21_{\mu}$-RD3	Computational model	0.552	0.193

Table S19: Buried Surface Area (BSA) for PIP-box residues from the cocrystal structures and computationally modelled peptides calculated using the PDBePISA server v1.52 (https://www.ebi.ac.uk/pdbe/pisa/). Å² / Buried area percentage

PIP-box Residue	***144^{P1}***	***145^{P2}***	***146^{P3}***	***147^{P4}***	***148^{P5}***	***149^{P6}***	***150^{P7}***	***151^{P8}***
Peptide								
p21 (1AXC, Gulbis 1996)	107.86 / 70	48.31/ 70	30.39 / 60	135.10 / 100	47.60 / 60	0 / 0	59.31 / 50	132.20 / 90
$p21_{\mu}$ (7KQ1)	98.61 / 70	46.23 / 70	31.97 / 60	140.61 / 100	34.23 / 40	0 / 0	66.67 / 50	130.92 / 90
$p21_{\mu}$-F150Y (7KQ0)	105.46 / 70	45.61 / 70	32.11 / 60	134.21 / 100	42.33 / 50	0 / 0	73.82 / 60	128.04 / 100
$p21_{\mu}$-S146R	93.41 / 70	46.73 / 70	68.11 / 50	142.96 / 100	32.99 / 40	0 / 0	74.02 / 60	133.52 / 90
$p21_{\mu}$-M147I	102.47 / 60	35.07 / 60	28.13 / 50	129.11 / 100	54.96 / 60	0 / 0	81.05 / 60	142.77 / 100
$p21_{\mu}$-D149E	98.26 / 60	50.34 / 80	29.24 / 50	140.27 / 100	42.59 / 50	0 / 0	75.43 / 60	136.21 / 100
$p21_{\mu}$-FY150/151YF	105.76 / 70	56.32 / 70	25.76 / 50	139.54 / 100	43.9 / 50	0 / 0	88.7 / 60	115.46 / 90
$p21_{\mu}$-PARG	37.43 / 30	60.13 / 80	60.46 / 50	126.43 / 100	50.59 / 60	0 / 0	66.62 / 50	117.12 / 100
$p21_{\mu}$-Pogo	73.05 / 60	71.12 / 60	53.08 / 50	131.07 / 100	62.18 / 60	0 / 0	83.77 / 60	120.27 / 90
$p21_{\mu}$-pol δ_{p66}	98.14 / 60	50.67 / 50	26.13 / 40	123.79 / 100	57.64 / 60	0 / 0	65.75 / 50	123.84 / 90
$p21_{\mu}$-pol ι	88.44 / 50	33.75 / 70	46.18 / 50	142.62 / 100	59.19 / 70	0 / 0	97.25 / 60	74.44 / 60
$p21_{\mu}$-RFC	76.16 / 40	86.28 / 60	23.01 / 40	138.71 / 100	85.43 / 50	0 / 0	62.59 / 60	96.61 / 70
$p21_{\mu}$-RD1	99.56 / 60	56.85 / 40	55.85 / 50	143.05 / 100	77.77 / 60	0 / 0	81.89 / 60	127.73 / 90
$p21_{\mu}$-RD2	72.88 / 50	57.05 / 90	65.92 / 50	136.97 / 100	52.52 / 50	0 / 0	76.75 / 50	104.72 / 100
$p21_{\mu}$-RD3	88.02 / 80	22.38 / 20	63.49 / 50	137.11 / 100	60.31 / 80	0 / 0	75.71 / 50	123.64 / 90

COMPARISON OF STRUCTURES TO NATIVE SEQUENCES

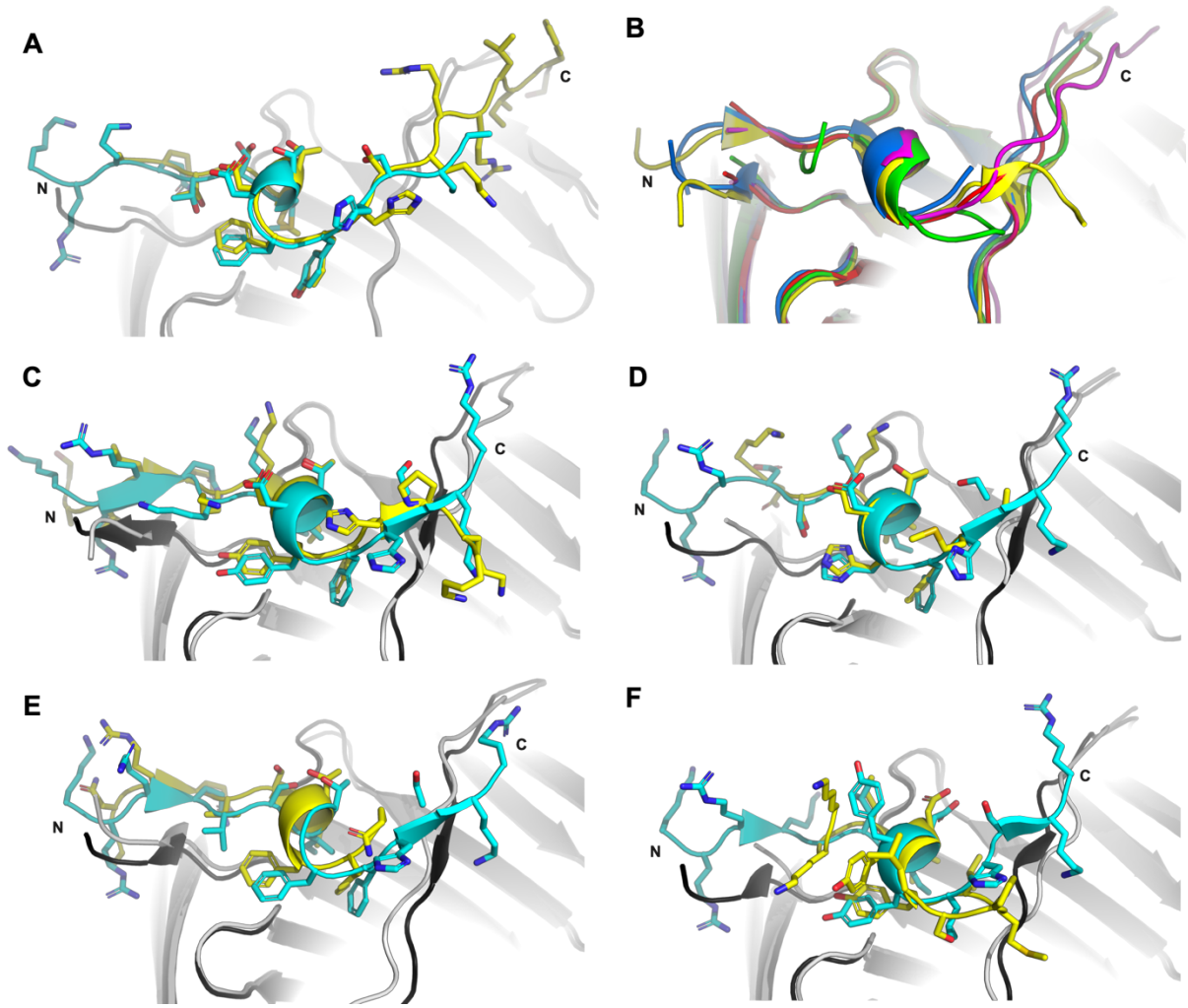

Figure S16: Overlaid structures of p21μ:PIP-box hybrid (PCNA, white; peptide, blue) and native PIP-box peptide (PCNA, black; peptide, yellow) shown in cartoon representation and side-chains of peptide as sticks. **A** p21μ (7KQ1) and $p21_{139-160}$ (1AXC) **B** Overlay of Native PIP-box peptides ($p21_{139-160}$ 1AXC, pink; PL 1VYJ, yellow; pol $\delta_{p66\ 452-466}$ 1U76, blue; $PARG_{402-420}$ 5MAV, red; pol ι $_{415-437}$ 2ZVM, green **C** p21μ-Pogo and PL (IVYJ) **D** p21μ-PARG and $PARG_{402-420}$ (5MAV) **E** p21μ-pol δ and pol $\delta_{p66\ 452-466}$ (1U76) **F** p21μ- pol ι and pol ι $_{415-437}$ (2ZVM).

Table S20: Root-mean-squared deviation (RMSD) values of alternative PIP-box modified peptides docked to monomer of hPCNA compared to the structures of their respective native peptides bound to hPCNA

Alternative PIP box mutant peptide docked to hPCNA	Structure of native peptide bound to hPCNA	RMSD value
$p21_{\mu}$-PARG	5MAV	0.496
$p21_{\mu}$-Pogo	1VYJ	0.646
$p21_{\mu}$-pol δ_{p66}	1U76	0.696
$p21_{\mu}$-pol ι	2ZVM	1.136

Table S21: Number of interactions for p21μ:hybrid peptides compared to native analogues determined from co-crystal or computationally modelled structures with RING server. For native structures the interactions are averaged over all subunit present in the pdb coordinate file.

					# Interactions					
Peptide	PDB ID:	Ref.	Affinity	# res	Total	PIP-box	Conserved	Non-conserved	Flanking	RING (3) session ID
p21 $_{139-160}$	1AXC	(4)	5.96 nM	22	60.67	25	9.33	15.67	35.67	5ef515200e9f94078ea226cb
$p21_{\mu}$	7KQ1		26.1 nM	15	30.67	23.67	16.67	7	7	5ef50f2b0e9f94078ea226bd
PL $_{1-16}$ [mutant]	1VYJ	(5)	100 nM	16	22.33	17.67	13.33	4.33	4.67	5ef515730e9f94078ea226cc
$p21_{\mu}$-Pogo			9.12 nM	15	34	24	16	5	10	5f3b224d0e9f94078ea22d01
pol $\delta_{p66\ 452-466}$	1U76	(6)	15.6 μM	15	30.33	24.33	17	7.33	6	5ef516b50e9f94078ea226cf
$p21_{\mu}$-pol δ_{p66}			268 nM	15	29	16	11	3	13	5f3b202a0e9f94078ea22cfb
PARG $_{402-420}$	5MAV	(7)	3.3 μM	19	26	19	4.83	14.17	7	5ef5164c0e9f94078ea226ce
$p21_{\mu}$-PARG			401 nM	15	24	15	8	4	9	5f3b1de50e9f94078ea22cf7
pol ι $_{415-437}$	2ZVM	(8)	0.39 μM	23	22.33	17.67	17.67	4.67	4.67	5ef515e00e9f94078ea226cd
$p21_{\mu}$-pol ι			1.42 μM	15	26	16	9	7	10	5f3b1e580e9f94078ea22cf8

REFERENCES

1. Anthis, N. J., and Clore, G. M. (2013) Sequence-specific determination of protein and peptide concentrations by absorbance at 205 nm. *Protein Sci.* **22**, 851-858
2. Wlodawer, A., Minor, W., Dauter, Z., and Jaskolski, M. (2013) Protein crystallography for aspiring crystallographers or how to avoid pitfalls and traps in macromolecular structure determination. *FEBS J.* **280**, 5705-5736
3. Piovesan, D., Minervini, G., and Tosatto, S. C. (2016) The RING 2.0 web server for high quality residue interaction networks. *Nucleic Acids Res.* **44**, W367-374
4. Gulbis, J. M., Kelman, Z., Hurwitz, J., O'Donnell, M., and Kuriyan, J. (1996) Structure of the C-Terminal Region of p21 WAF1/CIP1 Complexed with Human PCNA. *Cell* **87**, 297-306
5. Kontopidis, G., Wu, S.-Y., Zheleva, D. I., Taylor, P., McInnes, C., Lane, D. P., Fischer, P. M., and Walkinshaw, M. D. (2005) Structural and biochemical studies of human proliferating cell nuclear antigen complexes provide a rationale for cyclin association and inhibitor design. *Proc. Natl. Acad. Sci. U. S. A.* **102**, 1871-1876
6. Bruning, J. B., and Shamoo, Y. (2004) Structural and thermodynamic analysis of human PCNA with peptides derived from DNA polymerase-delta p66 subunit and flap endonuclease-1. *Structure* **12**, 2209-2219
7. Kaufmann, T., Grishkovskaya, I., Polyansky, A. A., Kostrhon, S., Kukolj, E., Olek, K. M., Herbert, S., Beltzung, E., Mechtler, K., Peterbauer, T., Gotzmann, J., Zhang, L., Hartl, M., Zagrovic, B., Elsayad, K., Djinovic-Carugo, K., and Slade, D. (2017) A novel non-canonical PIP-box mediates PARG interaction with PCNA. *Nucleic Acids Res.* **45**, 9741-9759
8. Hishiki, A., Hashimoto, H., Hanafusa, T., Kamei, K., Ohashi, E., Shimizu, T., Ohmori, H., and Sato, M. (2009) Structural basis for novel interactions between human translesion synthesis polymerases and proliferating cell nuclear antigen. *J. Biol. Chem.* **284**, 10552-10560